

Siphonophore Phylogeny

Catriona Munro¹, Stefan Siebert^{1,2}, Felipe Zapata^{1,3}, Mark Howison⁴, Alejandro Damian Serrano^{1,9}, Samuel H Church^{1, 5}, Freya Goetz^{1,6}, Phil Pugh⁷, Steven H.D. Haddock⁸, Casey W. Dunn^{1,9*}

¹ Department of Ecology and Evolutionary Biology, Brown University, Providence, RI 02912, USA

² Current address: Department of Molecular & Cellular Biology, University of California at Davis, Davis, CA 95616, USA

³ Current address: Department of Ecology and Evolutionary Biology, University of California Los Angeles, Los Angeles, CA 90095, USA

⁴ Brown Data Science Practice, Brown University, Brown University, Providence, RI 02912, USA

⁵ Department of Organismic and Evolutionary Biology, Harvard University, Cambridge, MA 02138, USA

⁶ Current address: Smithsonian Institution, National Museum of Natural History, Washington, DC 20560, USA

⁷ National Oceanography Centre, Southampton, SO14 3ZH, UK

⁸ Monterey Bay Aquarium Research Institute, Moss Landing, CA 95039, USA

⁹ Current address: Department of Ecology and Evolutionary Biology, Yale University, New Haven, CT 06520, USA

* Corresponding author, casey_dunn@brown.edu

Abstract

Introduction

Siphonophores are a group of 188 valid species within Hydrozoa (Cnidaria), the vast majority of which are members of the plankton (fig. 1). Siphonophores are colonial, and are composed of zooids that are each homologous to solitary animals, but are physiologically integrated (Totton and Bargmann 1965; Mackie et al. 1988; Dunn and Wagner 2006). Siphonophores differ significantly from all other colonial hydrozoans in terms of colony structure, development, and the degree to which they are functionally specialized (Beklemishev 1969; Cartwright and Nawrocki 2010). A siphonophore colony arises from a single embryo, which forms a protozooid and a growth zone from which other genetically identical zooids bud asexually (Carré 1967, 1969; Carré and Carré 1991, 1995). Each zooid arises in the same repeating species-specific pattern, and is functionally specialized for a particular task (e.g feeding, reproducing, swimming) (fig. 2) (Dunn and Wagner 2006).

Most siphonophores are planktonic, with the exception of one pleustonic species (*Physalia physalis*, Portuguese man of war) that lives at the interface of water and air, and a small clade of benthic siphonophores, the Rhodaliidae (Pugh 1983;).

Methods

This manuscript is an executable document computed directly from the data, providing an explicit and reproducible description of all findings. All scripts for the analyses are available in a git repository at https://github.com/caseywdunn/siphonophore_phylogeny_2017. The most recent commit at the time of the analysis presented here was 7cdbb6983a730c124a1e97f4be6dcf83e4de9c22.

Collecting

Collection data on all examined specimens, a description of the tissue that was sampled from the colony, collection mode, sample processing details, mRNA extraction methods, sequencing library preparation methods and sequencing details are summarized in supplementary table 1. Monterey Bay and Gulf of California specimens were collected by remotely operated underwater vehicle (ROV) or during blue-water scuba dives. *Chelophyes appendiculata* and *Hippopodius hippopus* specimens were collected in the bay of Villefranche-sur-Mer, France, during a plankton trawl on 04/13/11. Available physical vouchers have been deposited at the Museum of Comparative Zoology (Harvard University), Cambridge, MA, or had been previously deposited at the United States National Museum (Smithsonian Institution), Washington, DC. Accession numbers are given in supplementary table X. In cases where physical vouchers were unavailable we provide photographs to document species identity (table x).

Sequencing

When possible specimens were starved overnight in filtered seawater at temperatures close to ambient water temperatures at the time point of specimen collection (supplementary table 1). mRNA was extracted directly from tissue using a variety of methods (supplementary table x): Magnetic mRNA Isolation Kit (NEB, #S1550S), Invitrogen Dynabeads mRNA Direct Kit (Ambion, #61011), Zymo Quick RNA MicroPrep (Zymo #R1050), or from total RNA after Trizol (Ambion, #15596026) extraction and through purification using Dynabeads mRNA Purification Kit (Ambion, #61006)- in case of anticipated very small total RNA quantities, only a single round of bead purification was performed; or Trizol directly into the Illumina TruSeq Stranded Library Kit. Extractions were performed according to the manufacturer's instruction. Any resulting higher rRNA read counts were dealt with further downstream in the bioinformatics workflow. Libraries were prepared for sequencing using the Illumina TruSeq RNA Sample Prep Kit (Illumina, #FC-122-1001, #FC-122-1002), the Illumina TruSeq Stranded Library Prep Kit (Illumina, #RS-122-2101) or the NEBNext RNA Sample Prep Master Mix Set (NEB, #E6110S). We collected long read paired end Illumina data for *de novo* transcriptome assembly. In the case of large tissue inputs, libraries were sequenced separately for each tissue, subsequently subsampled and pooled *in silico*. Libraries were sequenced on the HiSeq 2000, 2500, and 3000 sequencing platforms (supplementary table 1). Summary statistics for expression libraries are given in Table 1.

Analysis

New data were analysed in conjunction with 13 publically available datasets, with a total number of 43 species. Sequence assembly, annotation, Maximum Likelihood (ML) phylogenetic analysis were conducted with the tool Agalma (Dunn et al. 2013), v. 1.00, and Bayesian Inference (BI) analyses were conducted using Phylobayes (Lartillot et al. 2009) v. 1.7a-mpi. Source code for all analysis steps, sequence alignments, sampled and consensus trees, and voucher information are available in a git repository https://github.com/caseywdunn/siphonophore_phylogeny_2017.

In the final analyses, we sampled 1,071 genes to generate a supermatrix with 60% occupancy and a length of 378,468 amino acids. Two outgroup species, *Atolla vanhoeffeni* and *Aegina citrea*, were removed from the final supermatrix and phylogeny due to low gene occupancy (gene sampling of 20.8% and 14.5% respectively in a 50% occupancy matrix with 2,203 genes). ML analyses were conducted on the unpartitioned supermatrix using the WAG+ Γ model of amino acid substitution, and bootstrap values were estimated using 1000 replicates. BI was conducted using two different CAT models, CAT-Poisson and CAT-GTR (Lartillot and Philippe 2004). Two independent MCMC chains were run under the CAT-GTR model, and four independent MCMC chains were run under the CAT-Poisson model. The CAT-GTR and CAT-poisson models did not converge after a long CPU time, and only the results from the CAT-poisson model are included here.

Morphological character data were obtained from the literature, or from direct observation of available voucher material.

Subsequent analyses were conducted in R and integrated into this manuscript with the `knitr` package. See Supplementary Information for R package version numbers.

Hypothesis testing

Results and Discussion

Sample collecting and sequencing

Species phylogeny

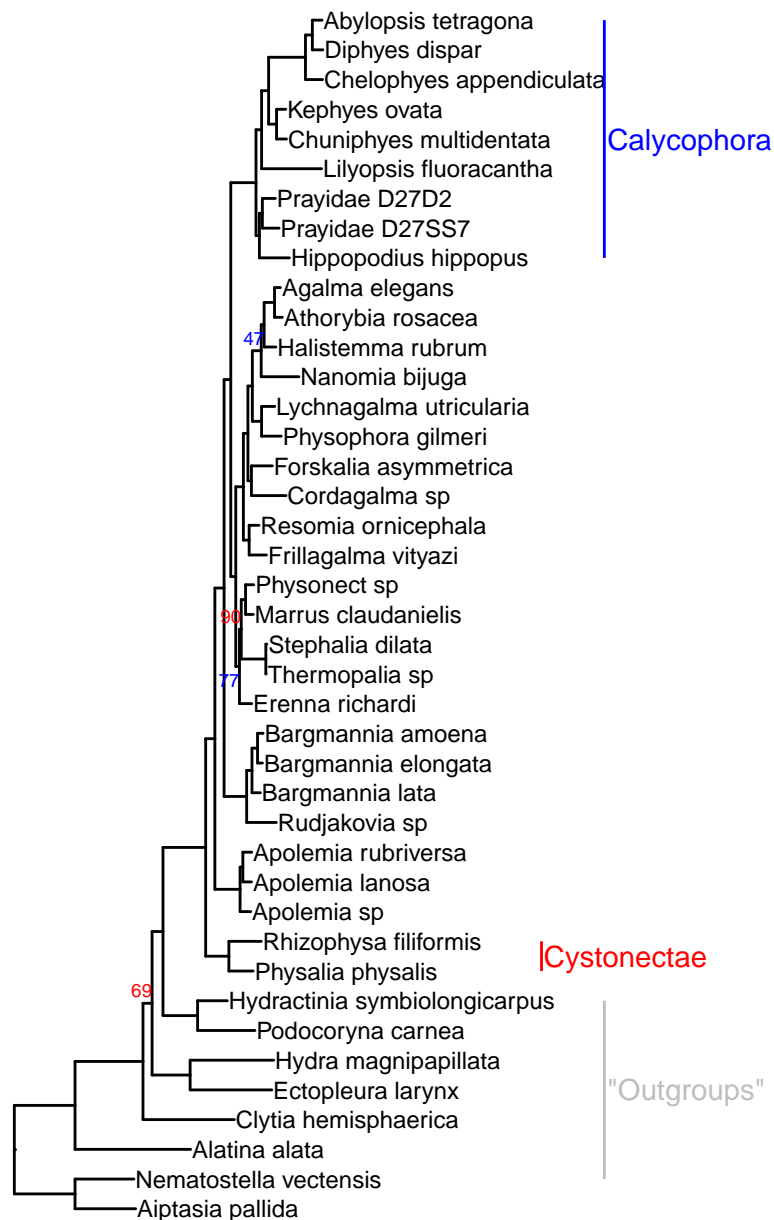


Figure 1: Phylogram of siphonophore relationships. Node labels indicate bootstrap support percent, unnumbered nodes have 100% support. The image was rendered with ggtree (Yu et al. 2016)

(XX This paragraph on sampling through *Agalma* analyses) The analyses presented here consider XXX siphonophore species and 8 outgroup species. This includes new data for XXX species. Summary stats on assemblies XX (Table XX). Matrix has XX genes, XX sites, and occupancy is XX.

(XX This paragraph summarizes phylogeny runs, apart from tree topology) Maximum likelihood analyses had 1000 replicates. We ran 4 phylobayes chains, and visual inspection of the traces indicated that a burn in of 400 trees was sufficient for all runs. This left 15847 trees in the posterior. XXConvergence...

These findings are entirely consistent with a previous analysis based on two genes (16S and 18S ribosomal RNA) (Dunn et al. 2005). Cystonectae is the sister group to the remaining siphonophores, and Calyphorae is nested within the paraphyletic “Physonectae”. In addition, multiple nodes that were not resolved in the previous two-gene analysis do receive strong support in this 1,071-gene transcriptome analysis. These findings include XXX.

Character Evolution

Siphonophores have evolved a fascinating diversity of morphological features, zooid types, life history traits, and habitats. Here we explore the evolutionary history of some of these features.

In our previous siphonophore phylogenetic analysis (Dunn et al. 2005) there were several characters left with equivocal evolutionary histories, due to unresolved relationships between physonects. With our current cladistic resolution, we were able to answer some of the questions left open:

Evolution of Monoecy

[Citation needed] noticed for the first time that some siphonophores were monoecious and others were dioecious. Our analyses in 2005 reconstructed this character and found a great amount of phylogenetic conservatism, with an unambiguous resolution of the MRCA (most recent common ancestor) as dioecious, and the appearance of monoecy in several taxa and clades (including Calyphorae) within the polytomy. Figure X shows the evolution of sex distribution in siphonophores under the current better-resolved tree model, and it strongly indicates that monoecy in siphonophores from a dioecious ancestor occurred twice, in the branch leading to Calyphorae and in the branch leading to Agalmatids (*sensu lato*). There is a small probability for an alternative scenario featuring a single gain of monoecy before the split of Calyphorae, with a subsequent derived shift back to dioecy in the *Marrus-Erenna* clade.

The Evolution of Zooid Types

One of the most striking aspects of siphonophore biology is their diversity of unique zooid types. Other colonial cnidarians (such as Hydractinia) and some bryozoans (example) have been found to have up to X different zooid types [Citation1, Citation 2]. The siphonophore genus *Forskalia* has 6 basic zooid types (pneumatophore, nectophore, gastrozooid, palpon, bract, and gonophore), and a total of 10 counting subtypes (4 types of bract, male & female gonophores). Diphyomorphs have more than 1 type of nectophore, while Cystonects have none. Here we reconstruct the evolutionary origins of the different zooid types on the present transcriptome tree.

Nectophores are retained modified medusae that Codonophora use for coordinated colony-level swimming. The nectosoma is the region of the colony that develops from the nectosomal growth zone. Unlike the siphosomal growth zone, the nectosoma does not bud gastrozooids, but nectophores (and in the case of *Apolemia*, also palpons). In fact, with the exception of *Physalia physalis* (which grows small nectophores near the gonodendra), siphonophore nectophores are exclusively found on the nectosoma. It is possible that the MRCA of siphonophores had a nectosoma, which has been lost on the branch leading to Cystonects. We cannot exclude with certainty the alternative hypothesis of a nectosoma-less ancestor followed by a gain of the nectosoma in the branch leading to the Codonophora. The nectosoma probably arose as a duplication of the siphosoma, followed by functional specialization in propelling the colony. The nectosoma has been lost within Codonophora in the genus *Athorybia*.

Following the colony development orientation framework presented in (citation), the nectosoma can be located in a dorsal or a ventral position. Our ancestral reconstructions for this character (Supp figure) show that

a ventrally-oriented nectosome was the ancestral form in siphonophores, and that a dorsal nectosome has evolved twice independently, in the branches leading to the Agalmatidae (sensu stricto) and the branch leading to the *Bargmannia* species. All Codonophora (with the exception of *Athorybia* species) have a nectosome, but the number and subtypes of nectophores present varies greatly between species. As shown in Figure X, most Codonophora presents the ancestral nectosome with multiple nectophores of the same subtype. However, Calyctophorans evolved a different system with just 2 nectophores of one type. This shift may be associated with the loss of the pneumatophore. Not all Calyctophorans remained with this arrangement. The Hippopodidae returned to bearing multiple identical nectophores, many of which are inactive and serve functions of defense (like a shell to retract in) and buoyancy. As in the rest of Calyctophorans, the Hippopodids only use 2 nectophores to propel the colony. Another interesting shift occurs in the branch leading to Diphyomorpha, where the 2 nectophores specialize into 2 subtypes, associated with a shift into a vertically aligned position and pointed bell shapes. The 2 types function together in a coupled hydrodynamic system that allows very fast escape responses (Mackie 1964).

Bracts are highly reduced zooids unique to siphonophores, but they are only present in the Codonophora. As with the nectosome, we have ambiguity determining whether the MRCA of siphonophores had bracts or not. The MRCA of Codonophora had only one bract subtype, which was lost in Hippopodidae and in *Gymnopræia lapislazula*. Bracts are functional for protection of the delicate zooids and to help maintain neutral buoyancy. Some calyctophorans are able to actively exclude sulphate ions in their bracts to adjust their buoyancy along the colony (Bidigare, R. R., & Biggs, D. C. (1980).

The ancestral siphonophore certainly had a pneumatophore (Supp Figure X). This unique zooid fills itself with gas, which helps the colony float and maintain its orientation in the water column. Recent evidence of neural arrangement in the pneumatophore of *Nanomia bijuga* (Church, 2013) suggests it could also gather information on relative pressure changes (and thus depth changes), helping regulate geotaxis. Despite its multiple biological functions, it was lost in the Calyctophorae and never gained again in that clade. Calyctophorans rely on the ionic balance of their gelatinous nectophores and bracts to retain posture and neutral buoyancy.

Palpons are modified mouthless gastrozooids used for digestion and circulation of the gastrovascular fluid. They were present in the MRCA of siphonophores (Supp Figure X), retained in most species, but lost twice independently in the branches leading to *Bargmannia* and Calyctophorae. These taxa might have found other avenues to effectively circulate nutrients across the colony.

The Gain and Loss of Tentilla

The most complex nematocyst batteries of Cnidaria can arguably be found among the siphonophores, hanging in regularly spaced tentacle side branches called tentilla. Most hydrozoans, including the clade that contains siphonophores, bear simple tentacles (tentacles with no side branches). It is still an open question whether the MRCA of Siphonophora had simple or branched tentacles. The only siphonophore genera regarded as lacking tentilla are *Physalia physalis* and *Apolemia* spp., and *Bathypheysa conifera*. Since *B. sibogae* is the only member of the *Rhizophysidae* (and of the *Bathypheysa* genus) lacking tentilla, we can safely assume this is a case of secondary loss. When we reconstruct the evolution of this character on the current phylogeny, we find that 70% of simulations support an MRCA bearing tentilla, with two independent losses leading to *Physalia* and *Apolemia*. However, this leaves a 30% support for a simple-tentacled MRCA followed by 2 independent gains of tentilla in the branches leading to *Rhizophysidae* and *{Bargmannia, Diphyes}*.

A key issue here is how we code for absence of tentilla, especially for the case of *Physalia physalis*. The tentacles of this species, when uncoiled, show very prominent, evenly spaced, bulging buttons which contain on their ectoderm all active and functionally arranged nematocysts used by the organism for prey capture. Siphonophore tentilla are complete diverticular branchings of the tentacle ectoderm, mesoglea, and gastrovascular canal (lined by endoderm). Hessinger & Ford 1988 (in the Biology of Nematocysts) described *Physalia*'s buttons as enclosing individual fluid-filled chambers connected by narrow channels to the tentacular canal, lined by endoderm. This suggests they are not just ectodermal swellings, but probably are reduced tentilla. When we code *Physalia physalis* as tentilla bearing, the results for the character reconstruction lead to a

more robust support for a tentilla-bearing MRCA followed by a single loss of tentilla in the branch leading to *Apolemiidae* (Figure 5b).

Siphonophore tentilla present an astounding diversity of sizes, shapes, colors, and nematocyst complements, and some have been observed to rapidly uncoil in contact with prey. Future research should explore the evolutionary history of these unique structures.

The Evolution of Vertical Habitat Use

Siphonophores are abundant predators in the pelagic realm, ranging from the surface (*Physalia physalis*) to bathypelagic depths (ref , *Bargmannia* sp 3888m VARS unpublished). While there are some pleustonic (*Physalia*) and benthic (*Rhodaliidae*) siphonophores, the phylogeny suggests the siphonophore MRCA was planktonic, as most extant taxa are. Some interesting questions arise from these facts, including 1) what was the bathymetric niche of the siphonophore MRCA, and 2) how did siphonophore's vertical habitat use of the water columns evolve along the phylogeny. Our results indicate a mesopelagic MRCA, with several convergent transition events to epipelagic and bathypelagic waters. There was only a single transition to benthic lifestyle on the stem of *Rhodaliidae*.

Discussion

The strong phylogenetic signal in the characters traditionally used for taxonomic diagnostics is a positive indicator of the applicability and unambiguity of these characters.

Conclusions

Acknowledgements

This work was supported by the National Science Foundation (DEB-1256695 and the Waterman Award). Sequencing at the Brown Genomics Core facility was supported in part by NIH P30RR031153 and NSF EPSCoR EPS-1004057. Data transfer was supported by NSF RII-C2 EPS-1005789. Analyses were conducted with computational resources and services at the Center for Computation and Visualization at Brown University, supported in part by the NSF EPSCoR EPS-1004057 and the State of Rhode Island. We also thank the MBARI crews and ROV pilots for collection of the specimens.

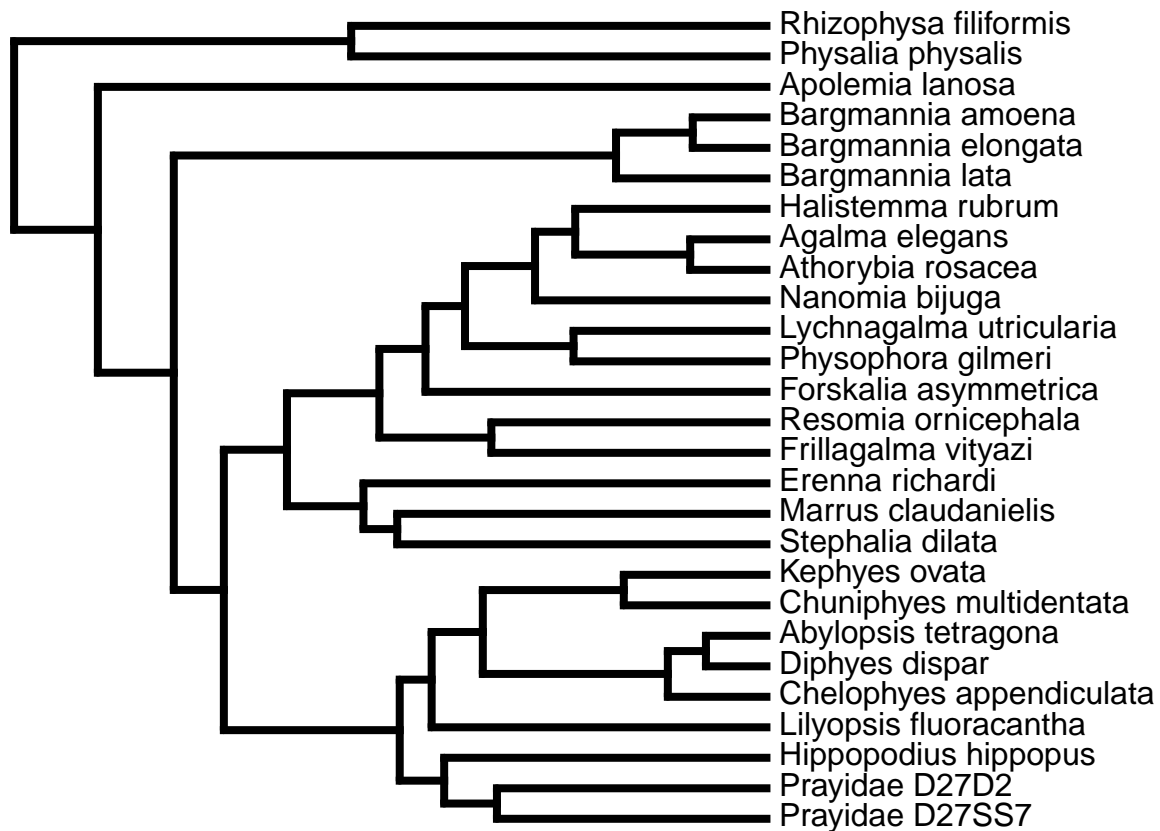
Supplementary Information

% latex table generated in R 3.4.1 by xtable 1.8-2 package % Fri Nov 3 16:00:19 2017

Table 1 (at the end of file): Summary statistics for libraries.

Supplementary Analyses

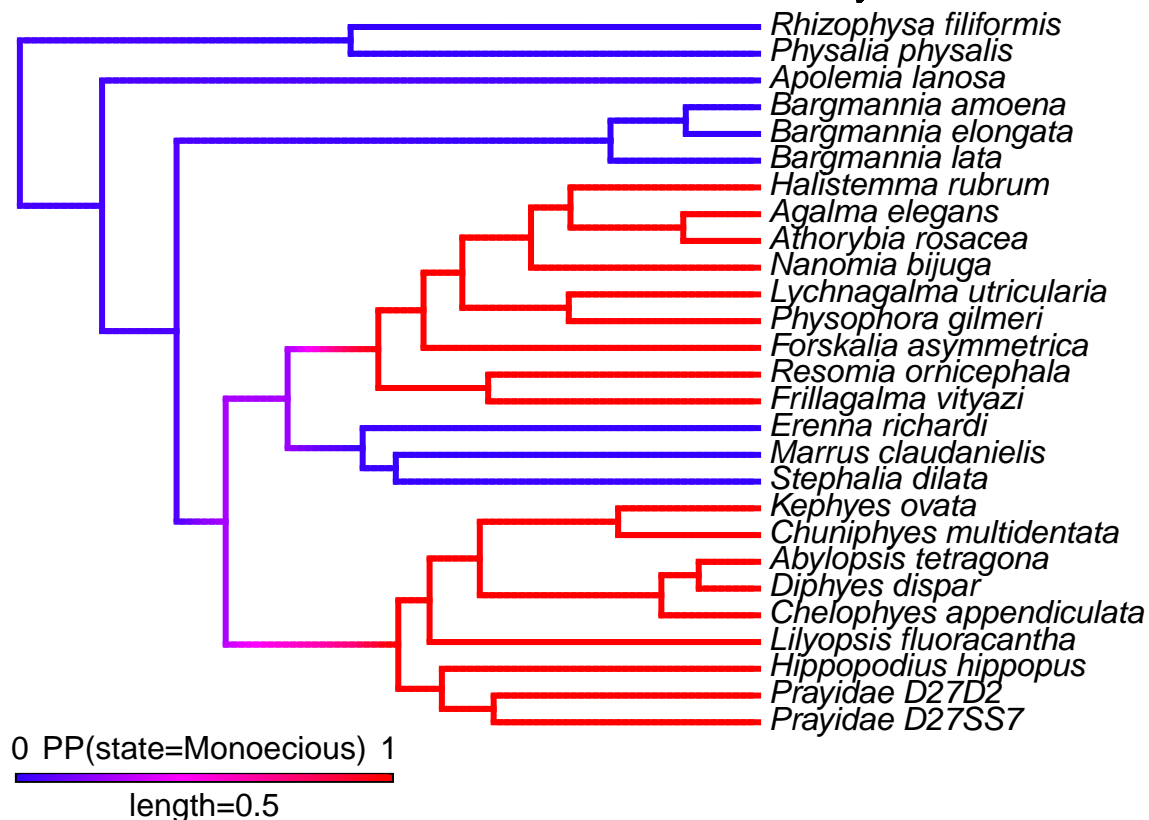
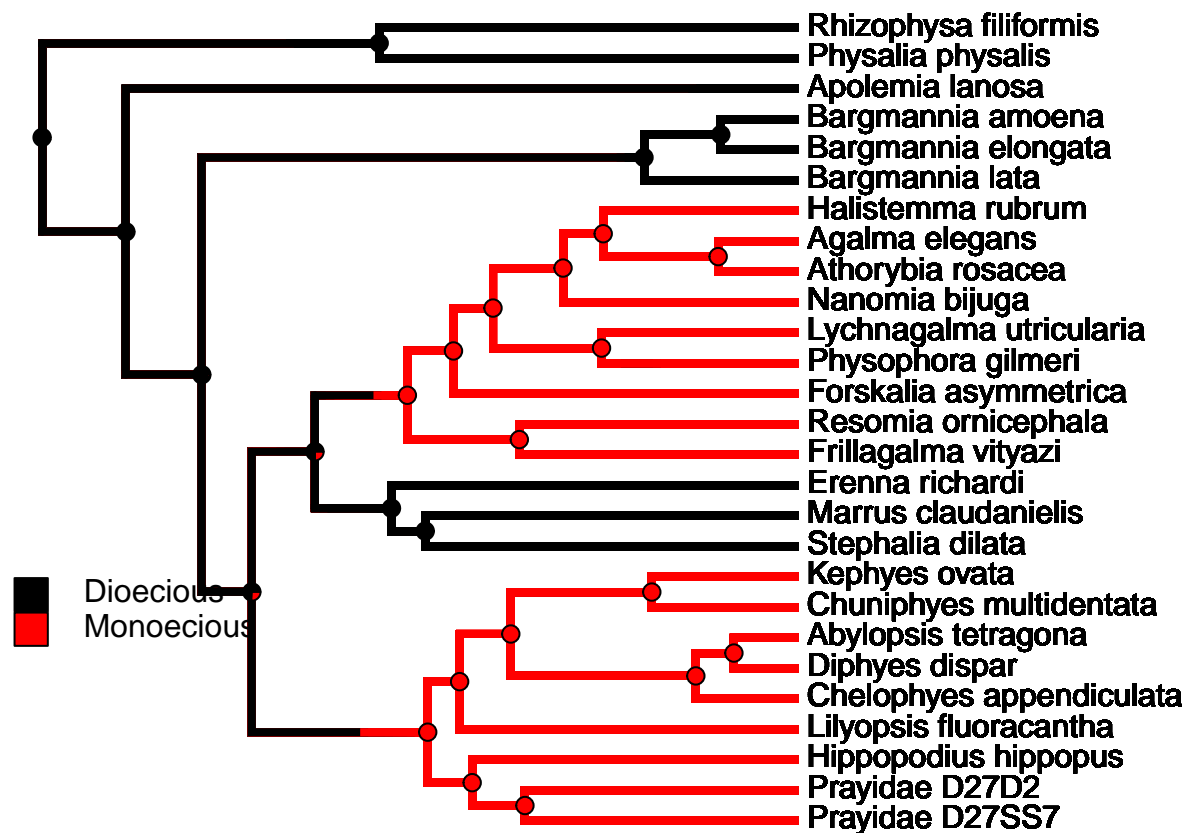
The Tree



```
## make.simmap is sampling character histories conditioned on the transition matrix
##
## Q =
##      0      1
## 0 -0.1892209  0.1892209
## 1  0.1892209 -0.1892209
## (estimated using likelihood);
## and (mean) root node prior probabilities
## pi =
##      0      1
## 0.5 0.5
```

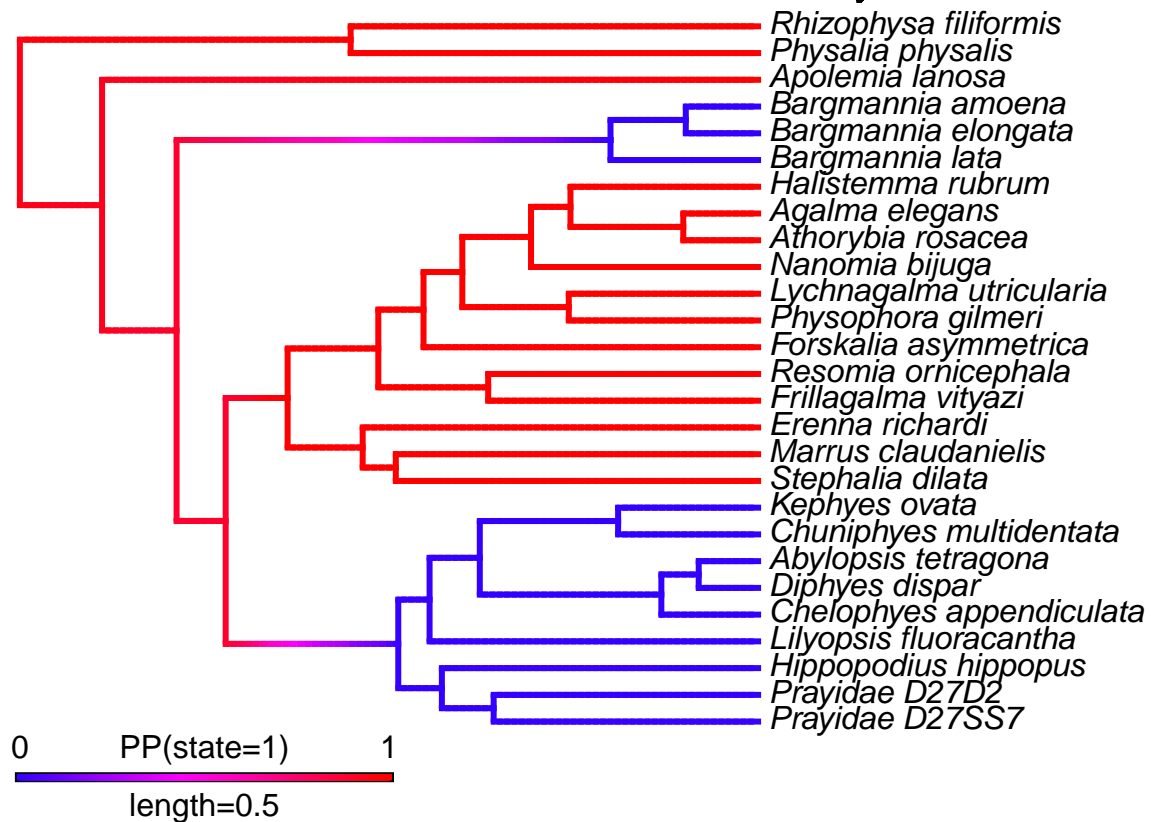
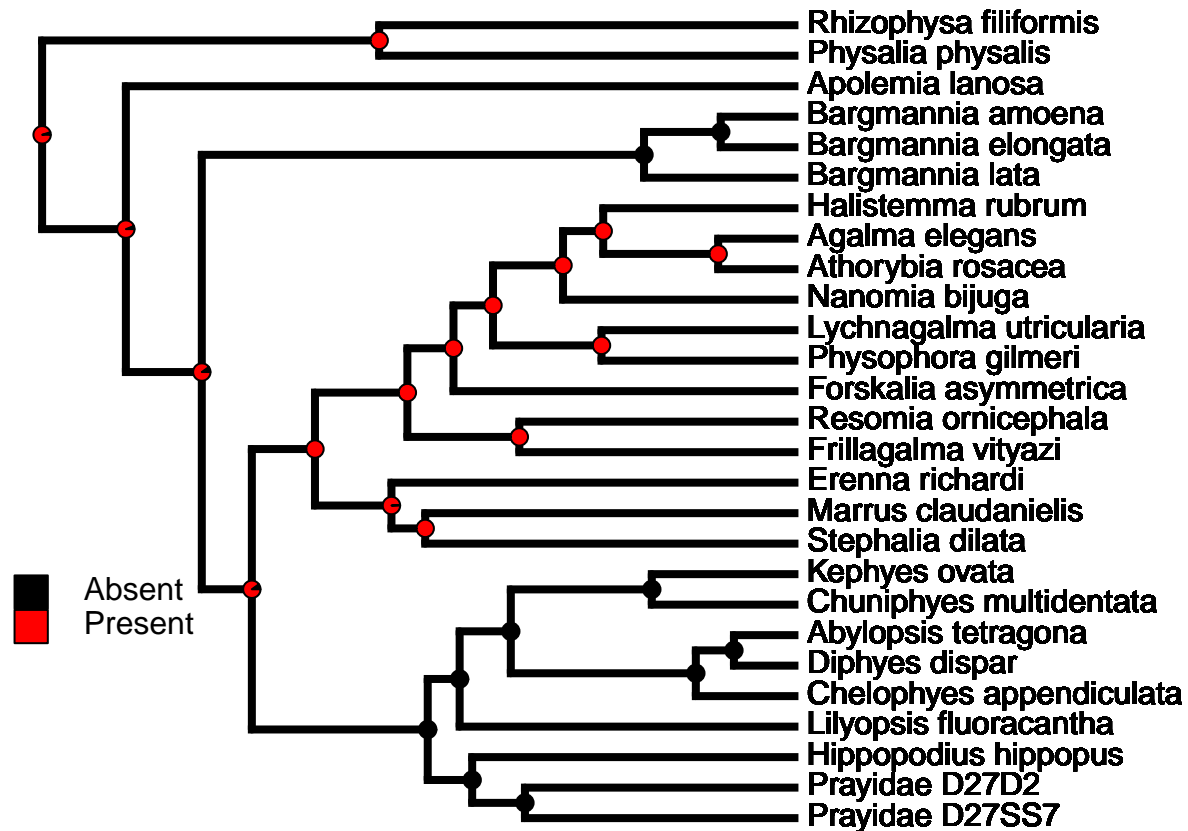
When we reconstruct the evolutionary history of different traits in siphonophore species, we obtain the following results:

SIMMAP Sex distribution



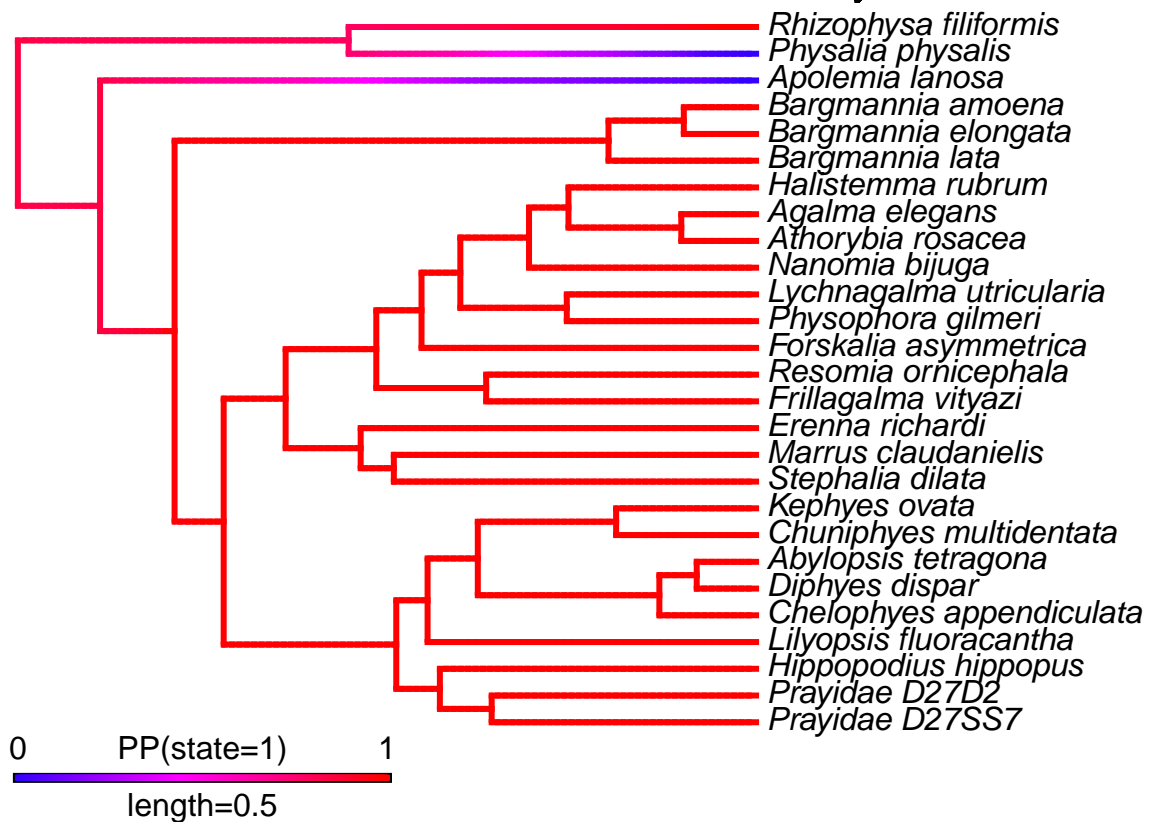
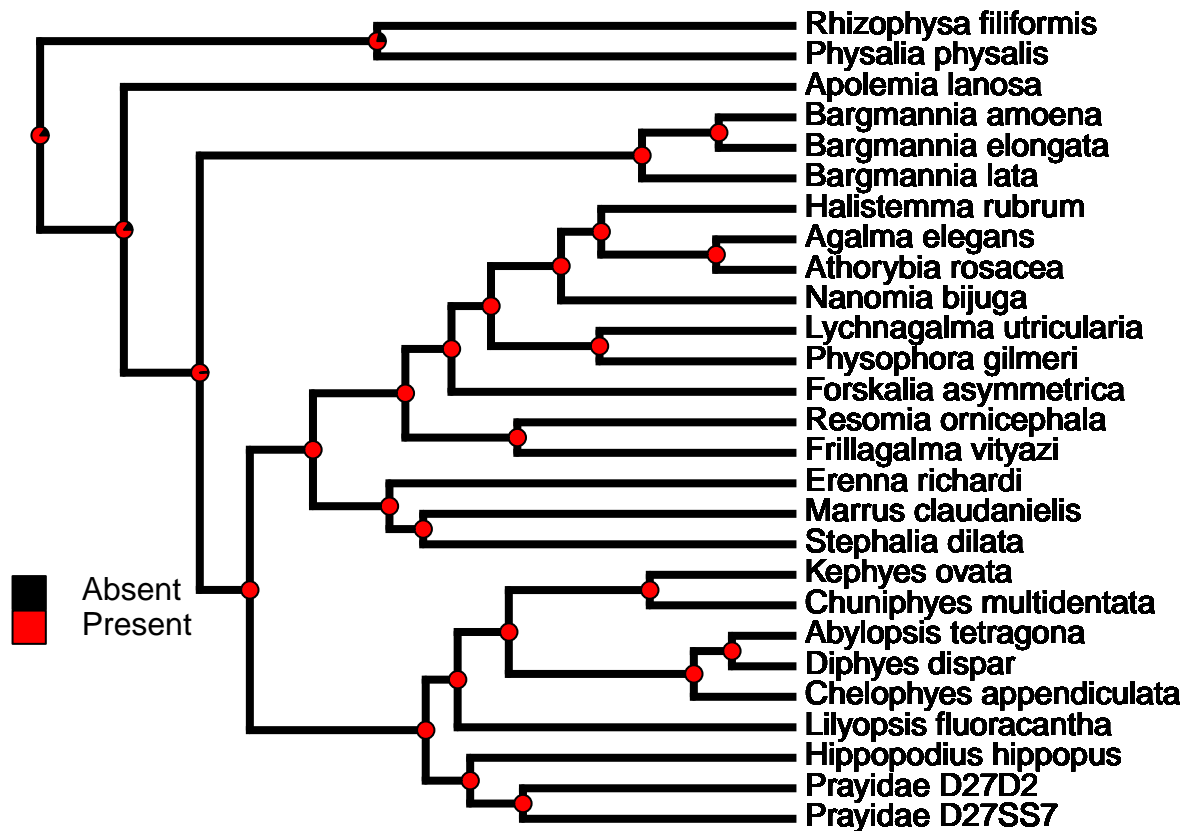
Posterior probabilities of states (0 Dioecious, 1 Monoecious).

SIMMAP Presence of palpons



Posterior probabilities of states (1 Present, 0 Absent).

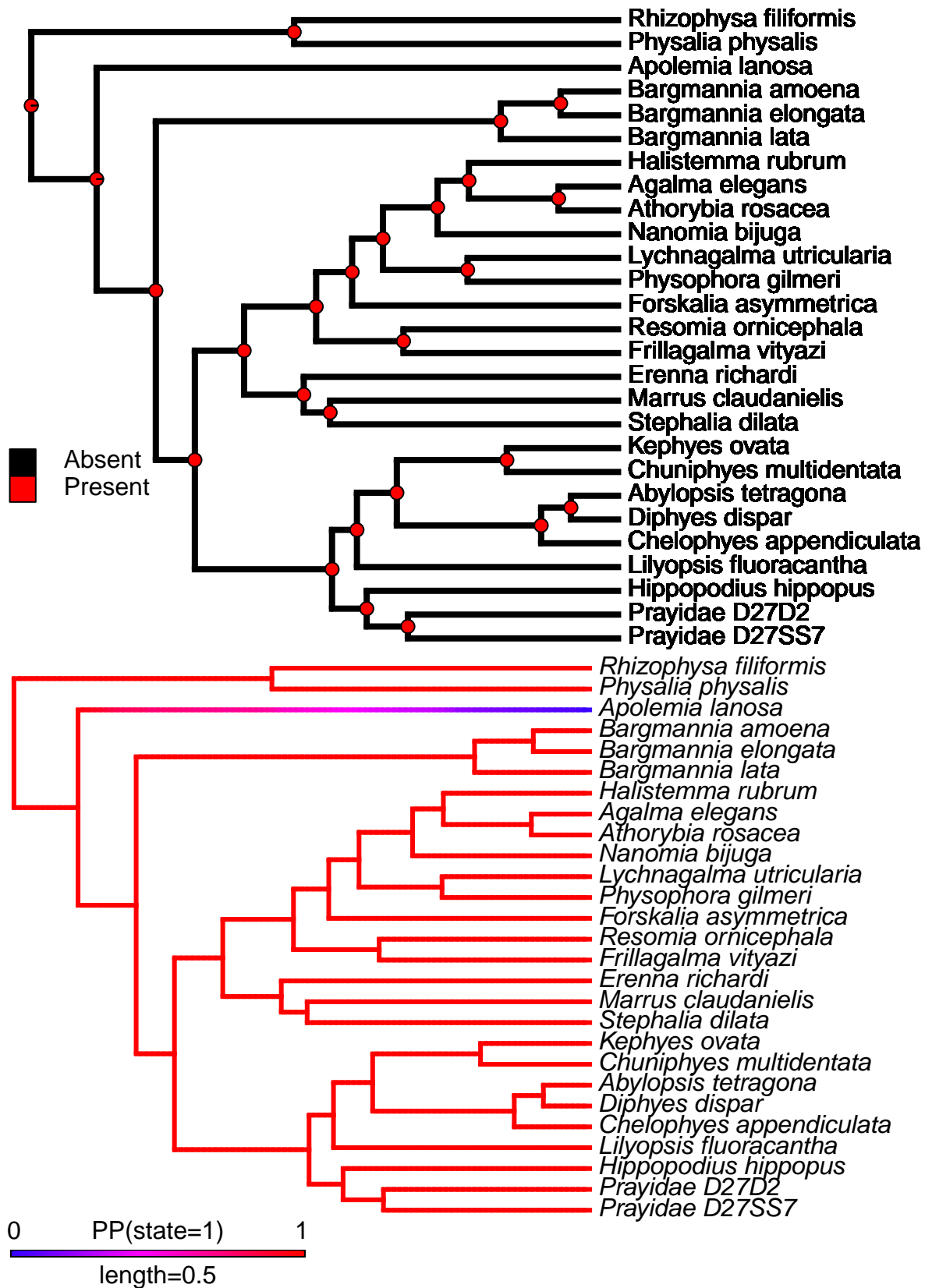
SIMMAP Presence of tentilla



Posterior probabilities of states (1 Present, 0 Absent).

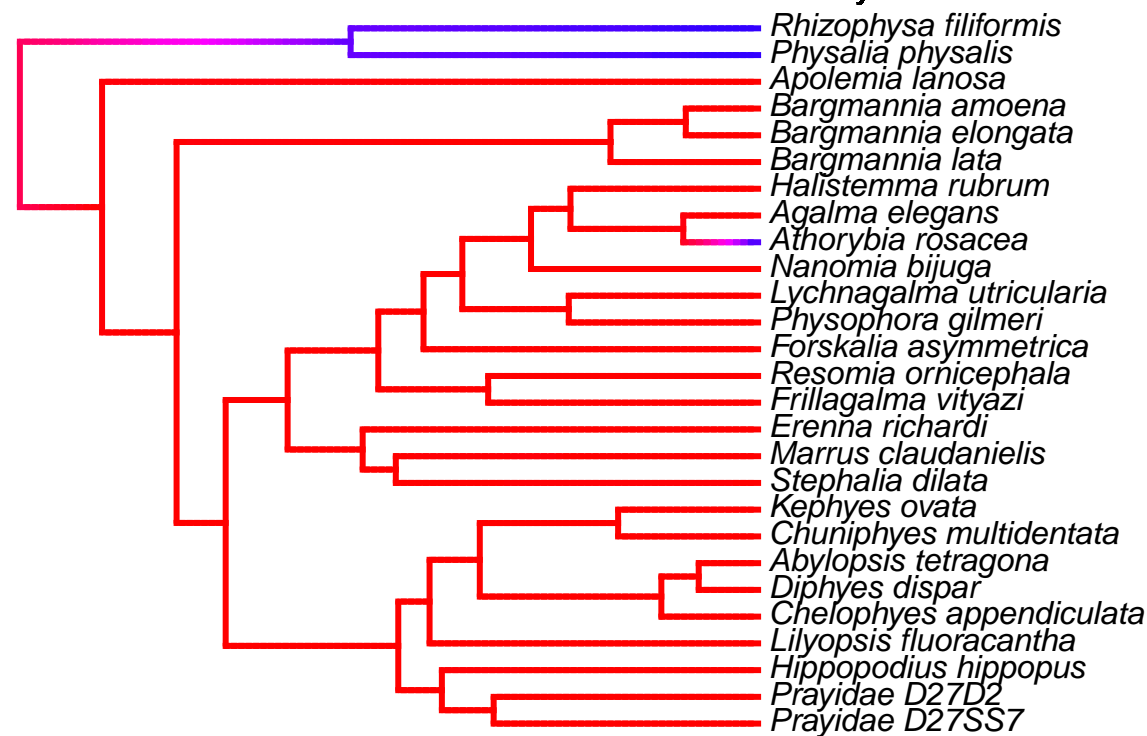
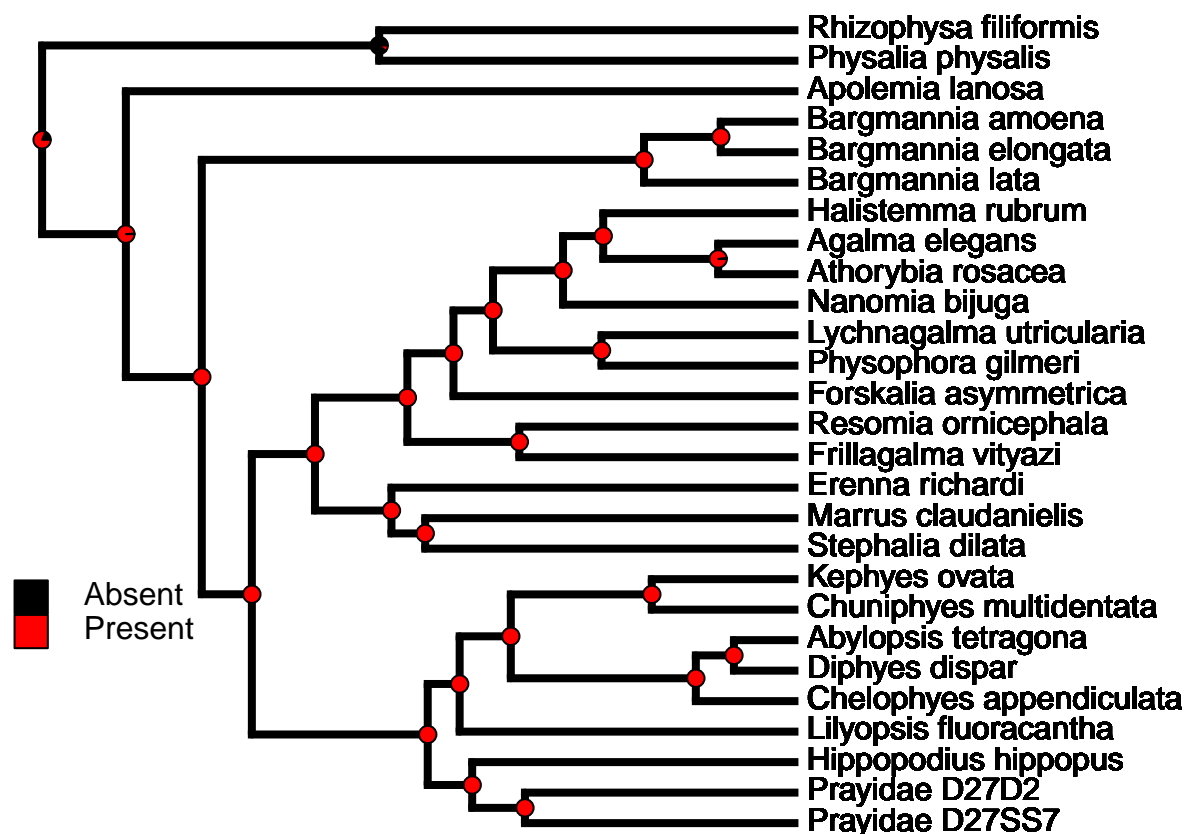
Physalia physalis may have reduced tentilla, which would indicate there was only one loss of tentilla at the branch leading to *Apolemia*.

SIMMAP Presence of tentilla - *Physalia* corrected



Posterior probabilities of states (1 Present, 0 Absent).

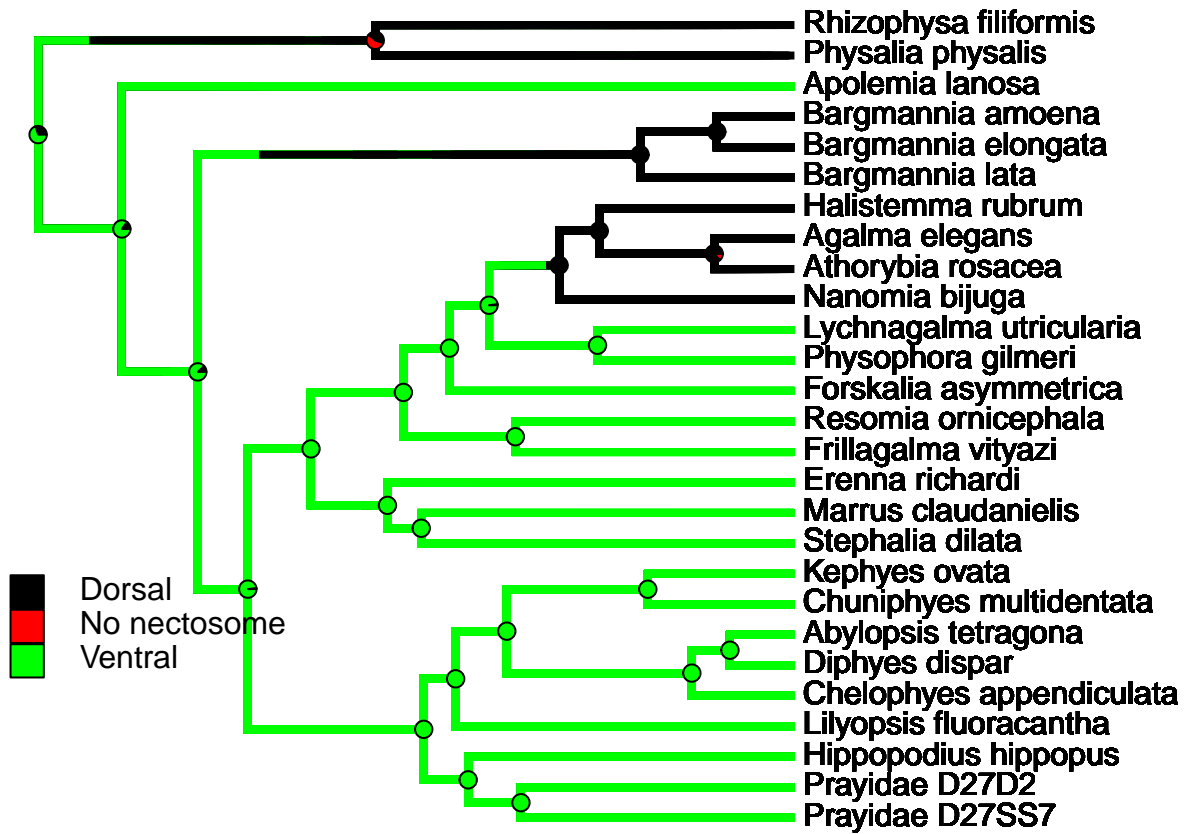
SIMMAP Presence of Nectophores



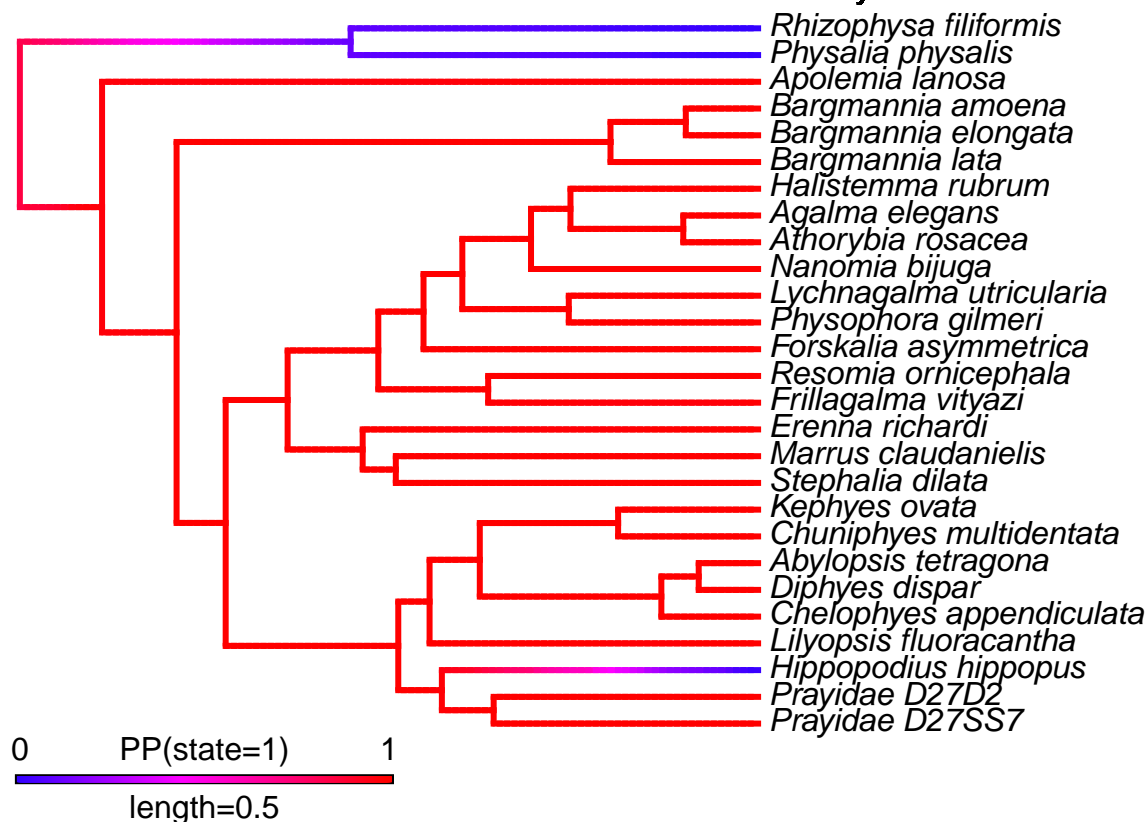
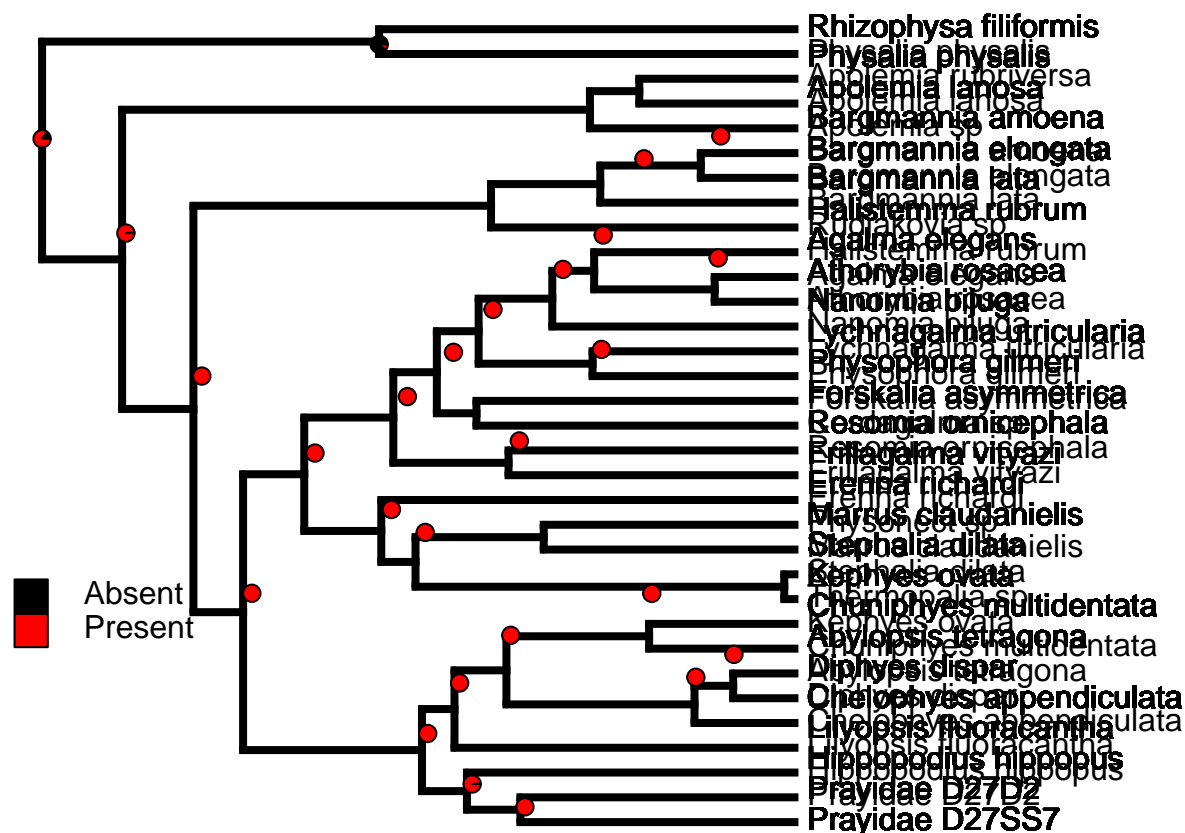
probabilities of states (1 Present, 0 Absent).

Posterior

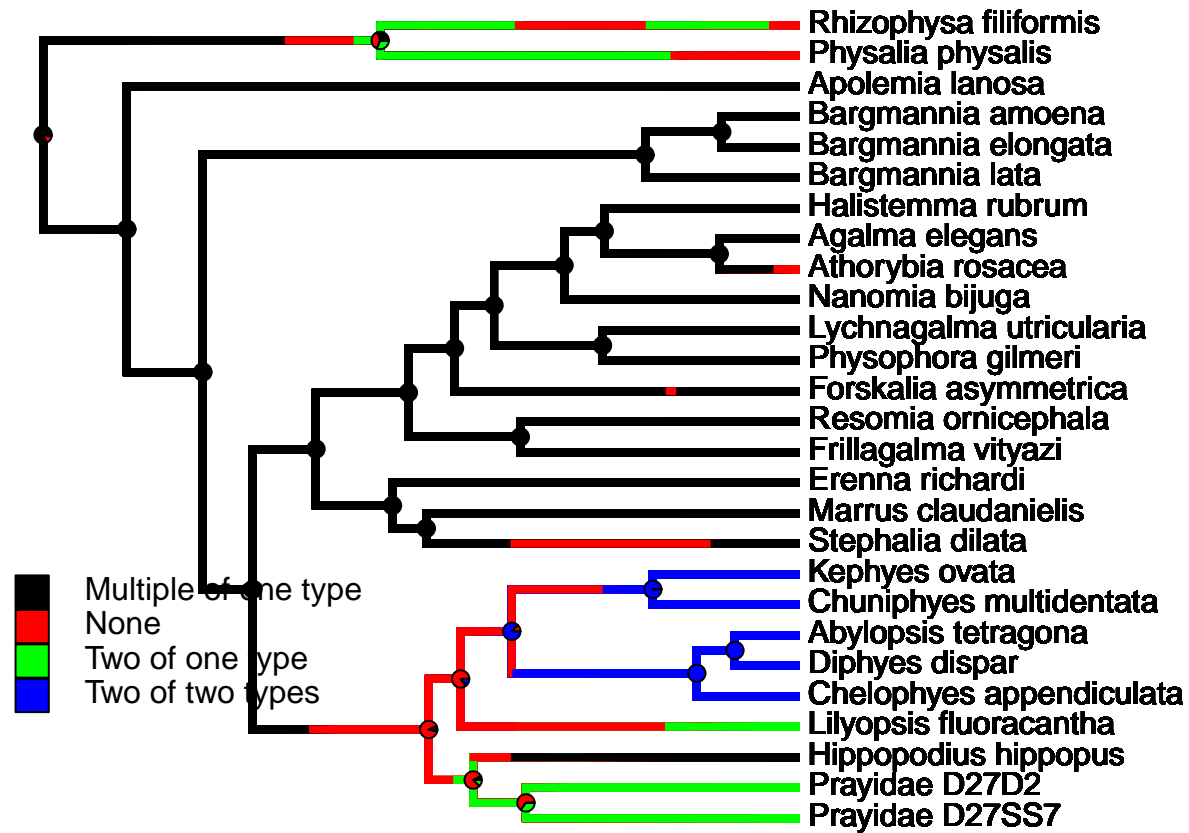
SIMMAP Position of Nectosome



SIMMAP BRACTS:

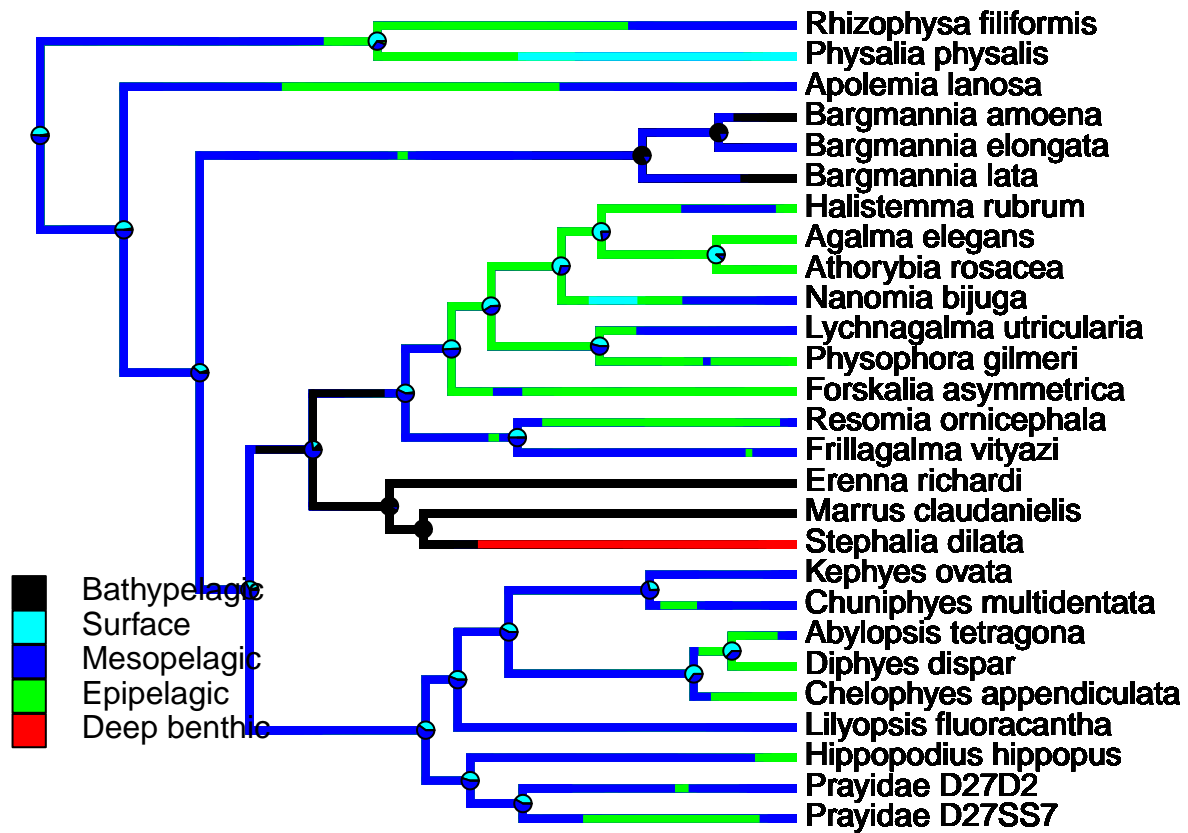


SIMMAP Nectophore number and types



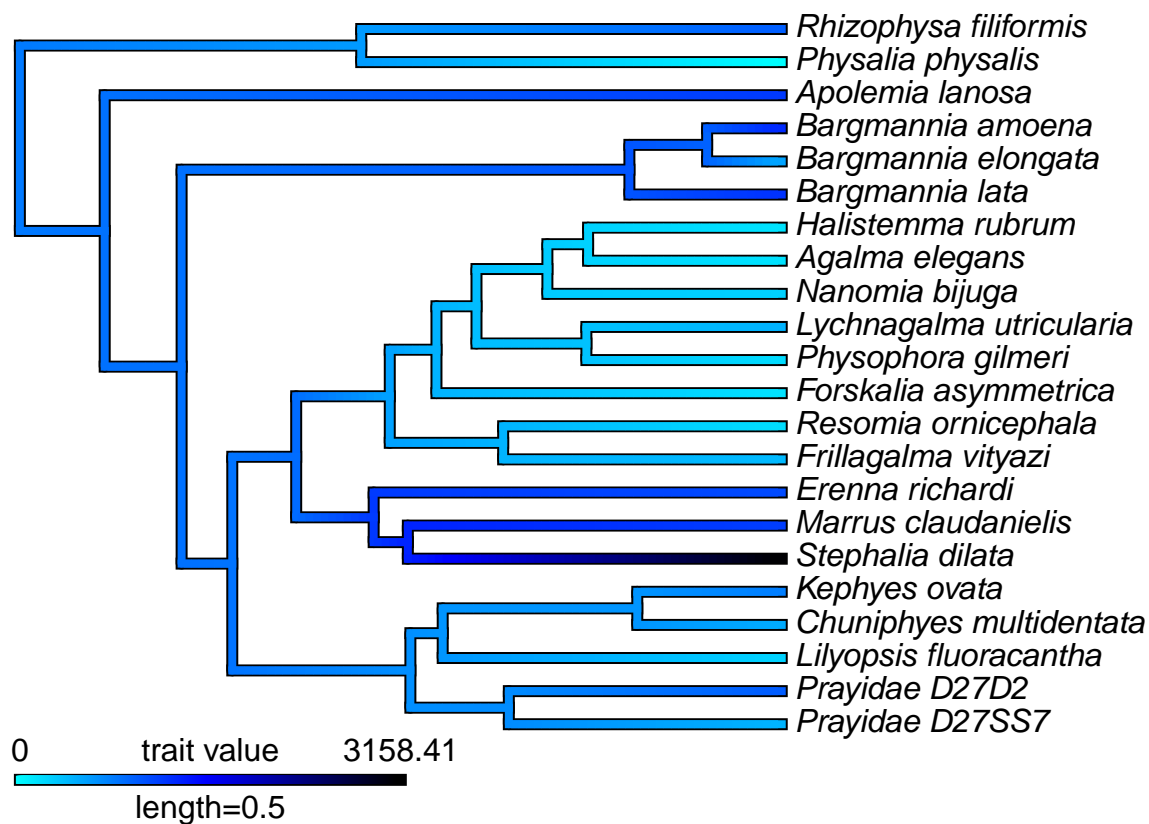
Posterior probabilities of states (1 Present, 0 Absent). It is not clear whether or not the stem group of siphonophores had a pneumatophore.

SIMMAP Habitat

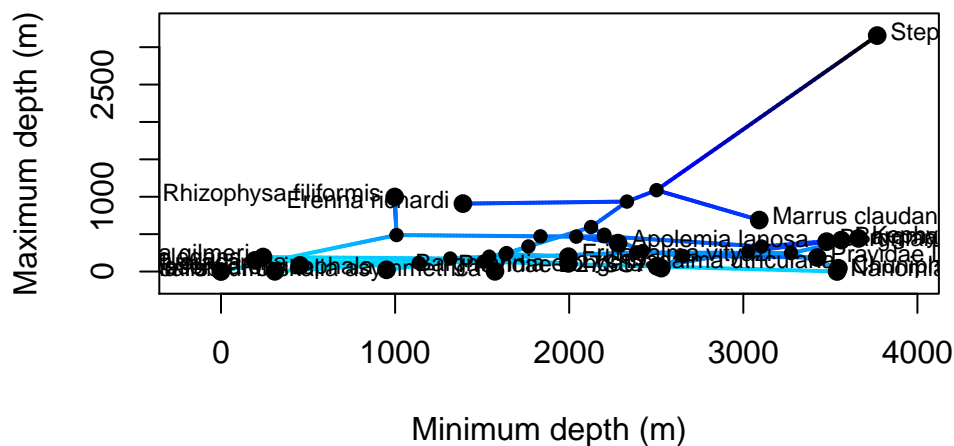


Continuous traits: Brownian motion reconstructions

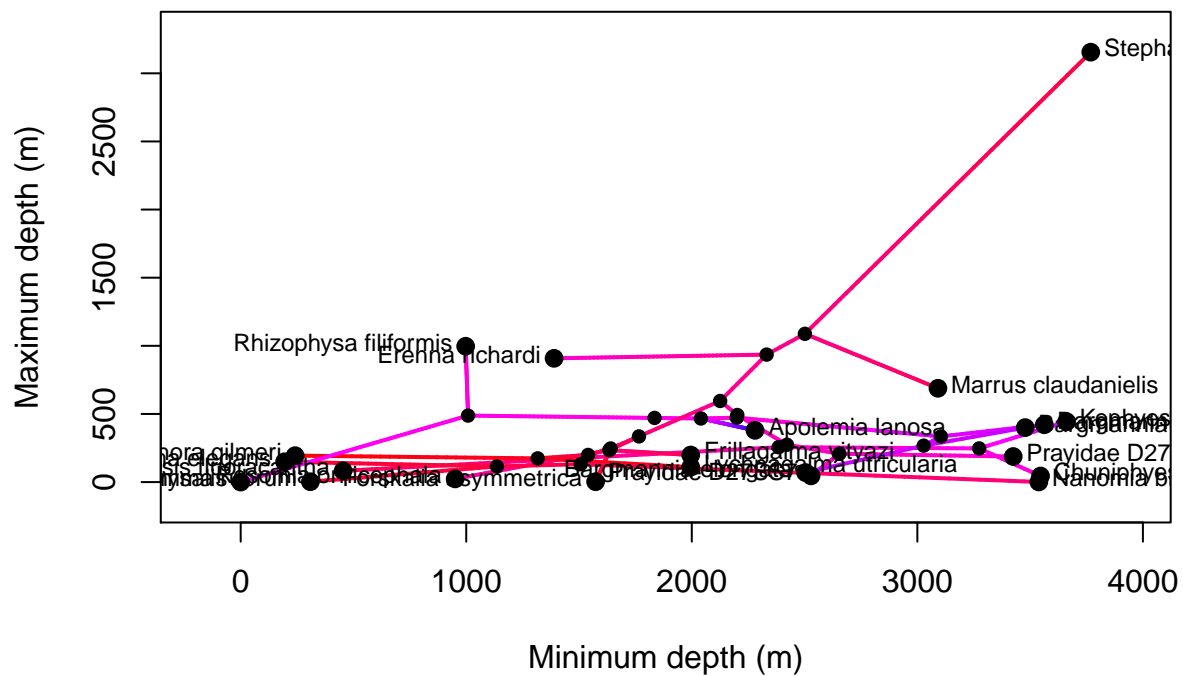
Median depth reconstruction:



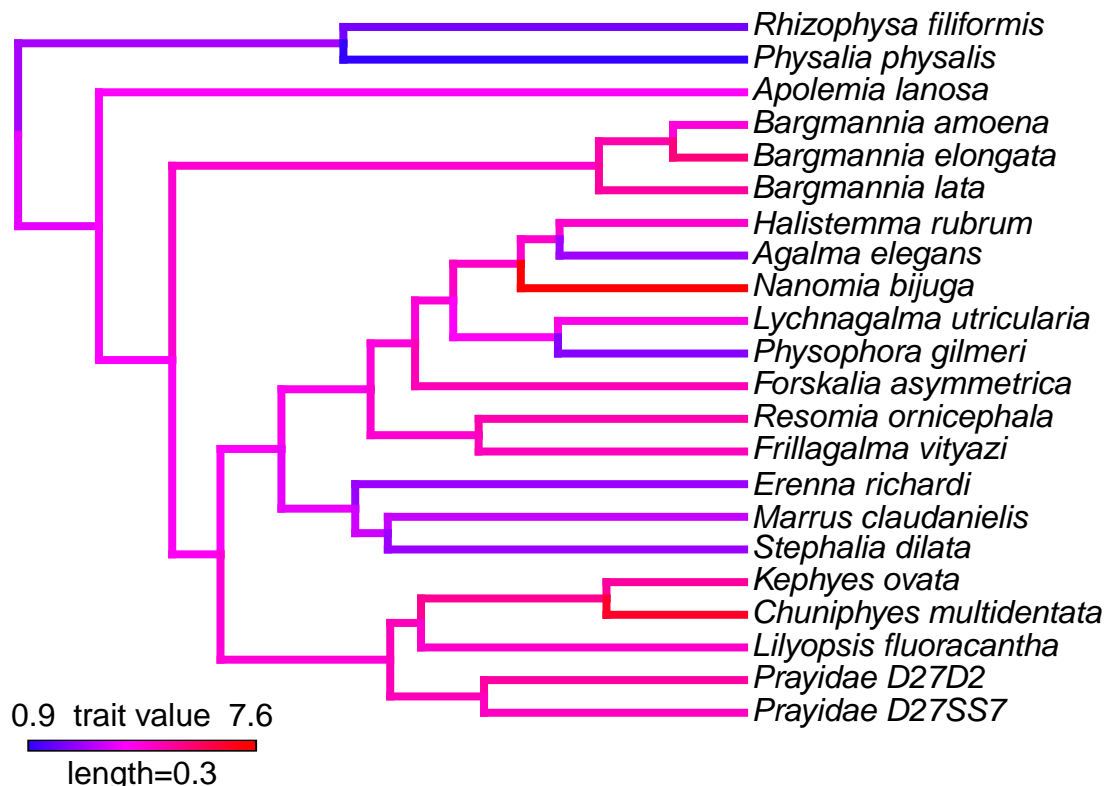
Bathymetrics phylomorphospace



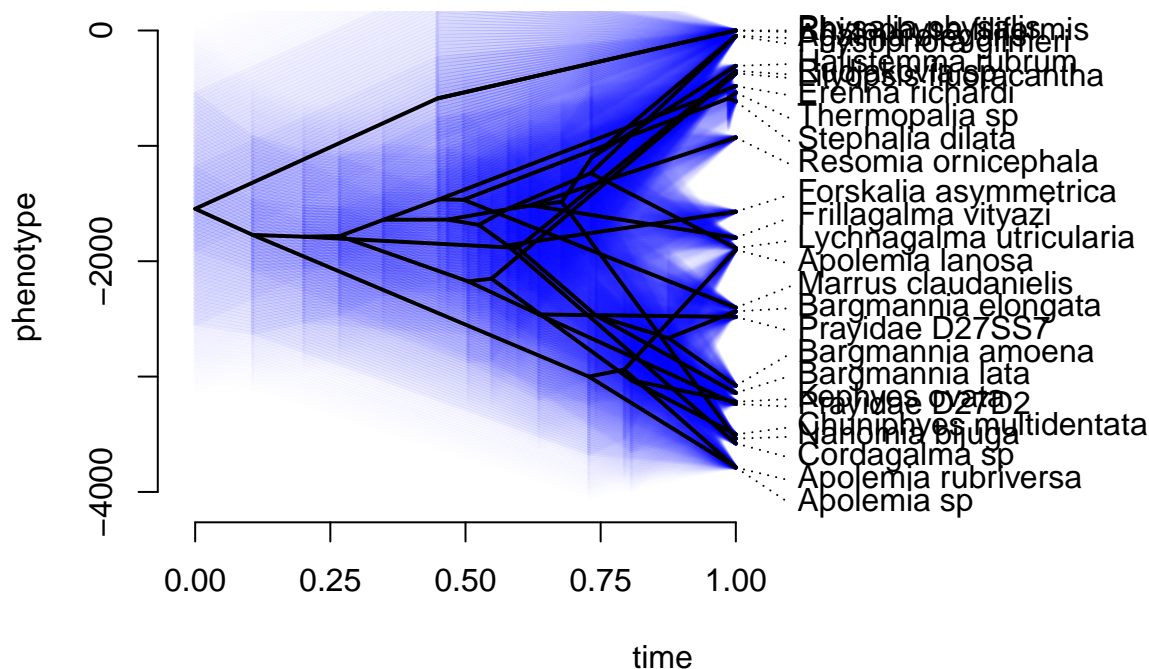
Bathymetrics phylomorphospace with time from root as color



Abundance of each taxon in the Monterey Bay sampling site

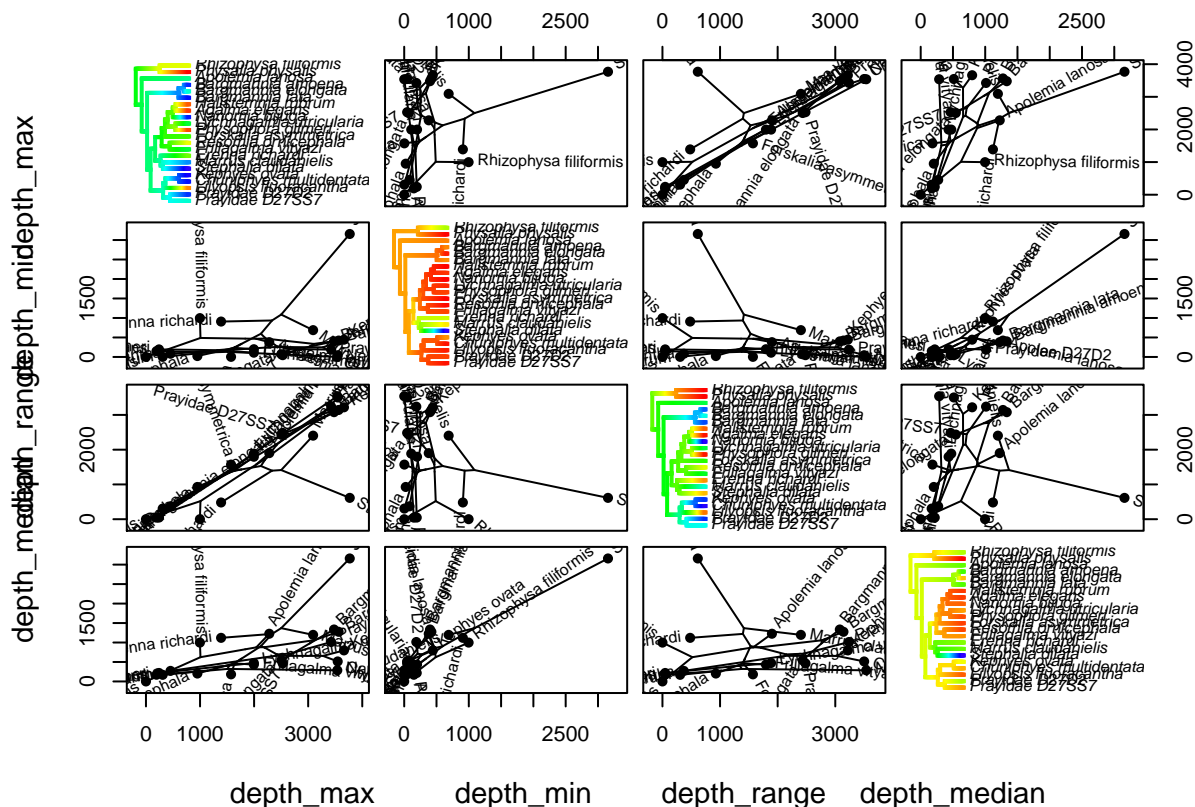


Uncertainty inclusive traitgram for depth range



Bathymetrics scattergram array

Computing multidimensional phylogenetic scatterplot matrix...



Distribution of sex across siphonophore taxa

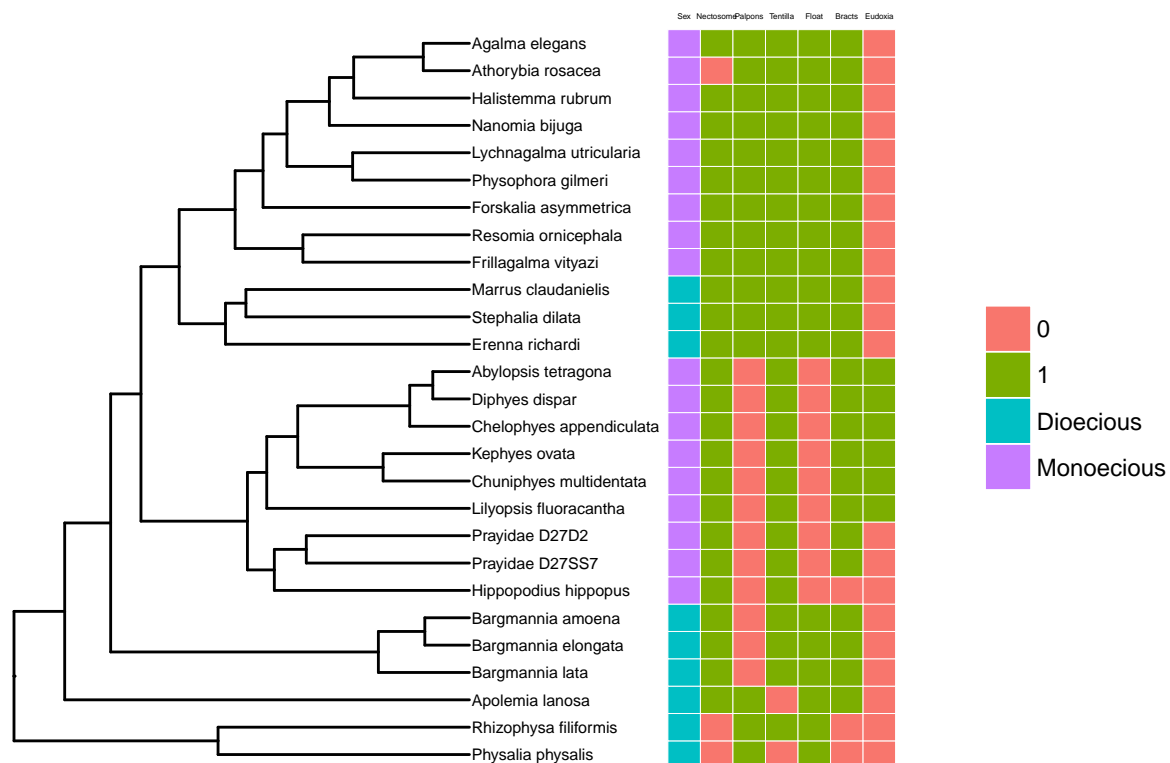
Tentilla presence across siphonophore taxa

Palpon presence across siphonophore taxa

Overview grid of main binary traits

##	Sex	Nectosome	Palpons	Tentilla
## Prayidae D27SS7	Monoecious	1	0	1
## Prayidae D27D2	Monoecious	1	0	1
## Hippopodius hippopus	Monoecious	1	0	1
## Lilyopsis fluoracantha	Monoecious	1	0	1
## Chelophyes appendiculata	Monoecious	1	0	1
## Diphyes dispar	Monoecious	1	0	1
## Abylopsis tetragona	Monoecious	1	0	1
## Chuniphyes multidentata	Monoecious	1	0	1
## Kephyes ovata	Monoecious	1	0	1
## Stephalia dilata	Dioecious	1	1	1
## Marrus claudanielis	Dioecious	1	1	1
## Erenna richardi	Dioecious	1	1	1
## Frillagalma vityazi	Monoecious	1	1	1
## Resomia ornicephala	Monoecious	1	1	1
## Forskalia asymmetrica	Monoecious	1	1	1
## Physophora gilmeri	Monoecious	1	1	1
## Lychnagalma utricularia	Monoecious	1	1	1
## Nanomia bijuga	Monoecious	1	1	1
## Athorybia rosacea	Monoecious	0	1	1
## Agalma elegans	Monoecious	1	1	1
## Halistemma rubrum	Monoecious	1	1	1
## Bargmannia lata	Dioecious	1	0	1
## Bargmannia elongata	Dioecious	1	0	1
## Bargmannia amoena	Dioecious	1	0	1
## Apolemia lanosa	Dioecious	1	1	0
## Physalia physalis	Dioecious	0	1	0
## Rhizophysa filiformis	Dioecious	0	1	1
##	Pneumatophore	Bracts	Eudoxia	
## Prayidae D27SS7	0	1	0	
## Prayidae D27D2	0	1	0	
## Hippopodius hippopus	0	0	0	
## Lilyopsis fluoracantha	0	1	1	
## Chelophyes appendiculata	0	1	1	
## Diphyes dispar	0	1	1	
## Abylopsis tetragona	0	1	1	
## Chuniphyes multidentata	0	1	1	
## Kephyes ovata	0	1	1	
## Stephalia dilata	1	1	0	
## Marrus claudanielis	1	1	0	
## Erenna richardi	1	1	0	
## Frillagalma vityazi	1	1	0	
## Resomia ornicephala	1	1	0	
## Forskalia asymmetrica	1	1	0	

## Physophora gilmeri	1	1	0
## Lychnagalma utricularia	1	1	0
## Nanomia bijuga	1	1	0
## Athorybia rosacea	1	1	0
## Agalma elegans	1	1	0
## Halistemma rubrum	1	1	0
## Bargmannia lata	1	1	0
## Bargmannia elongata	1	1	0
## Bargmannia amoena	1	1	0
## Apolemia lanosa	1	1	0
## Physalia physalis	1	0	0
## Rhizophysa filiformis	1	0	0



Phylogenetic signal in the character data

Agnostic branch length tree generation:

Phylogenetic signal in Binary Traits

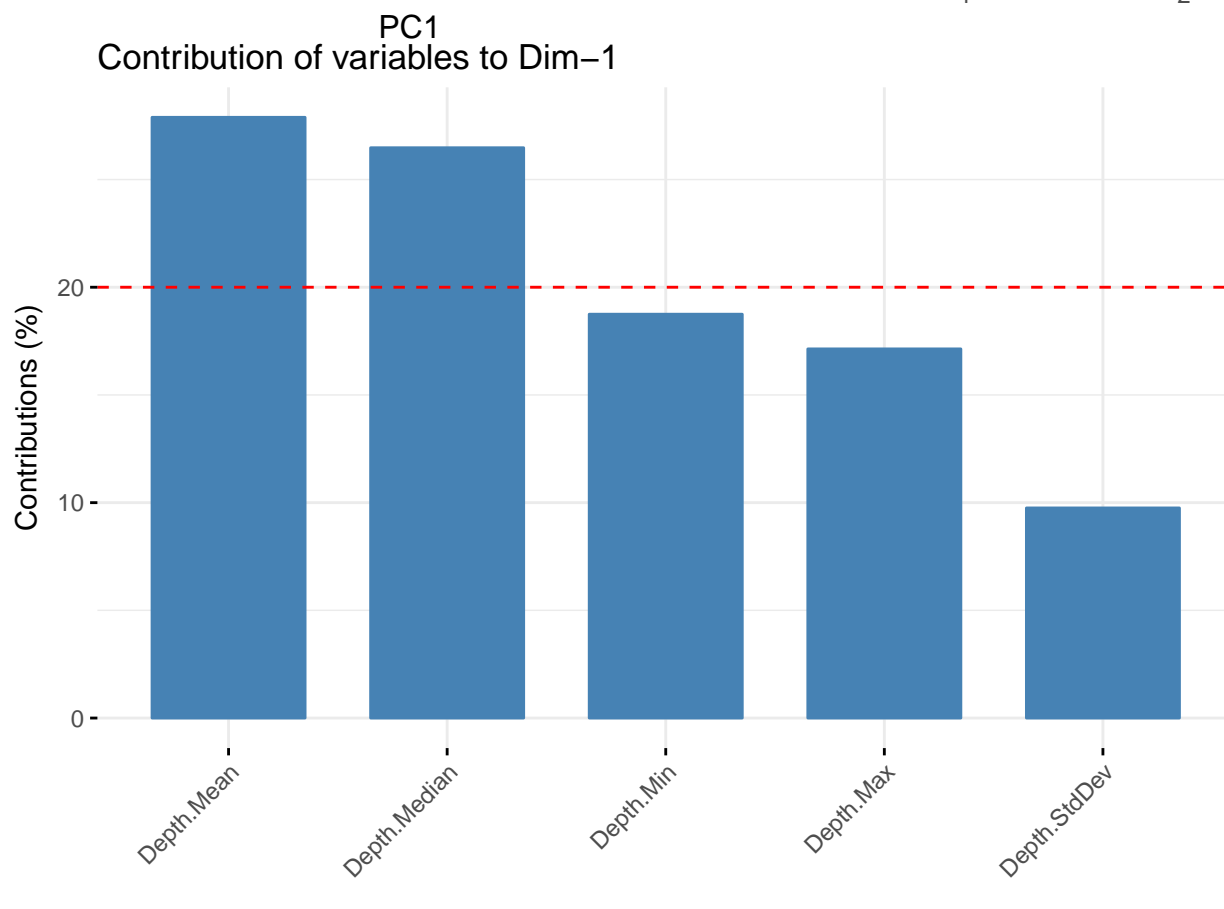
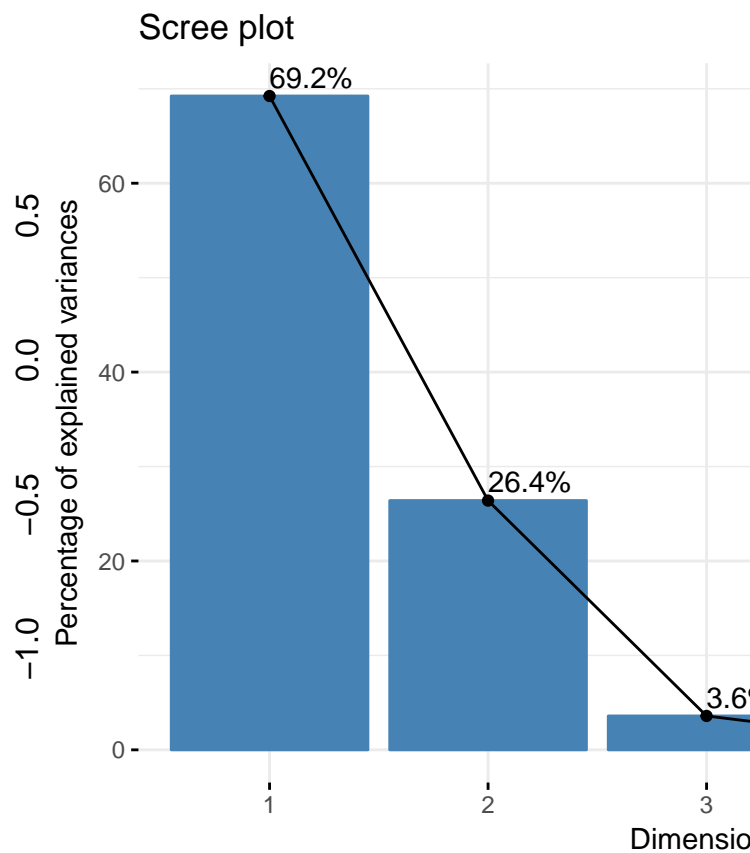
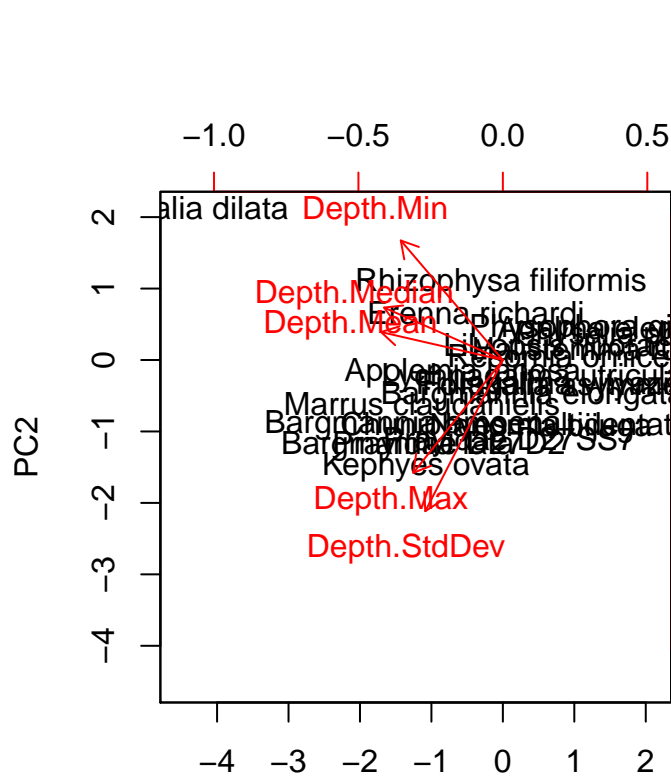
##	K	PIC.variance.obs	PIC.variance.rnd.mean
## Nectosome	0.6773278	0.26773672	0.3507614
## Palpons	3.3888711	0.10615819	0.8624120
## Tentilla	2.1806411	0.07424251	0.2434057
## Pneumatophore	3.9000634	0.08521926	0.7768665
##	PIC.variance.P	PIC.variance.Z	
## Nectosome	0.319	-0.6680884	
## Palpons	0.001	-4.2989067	
## Tentilla	0.003	-1.5642236	

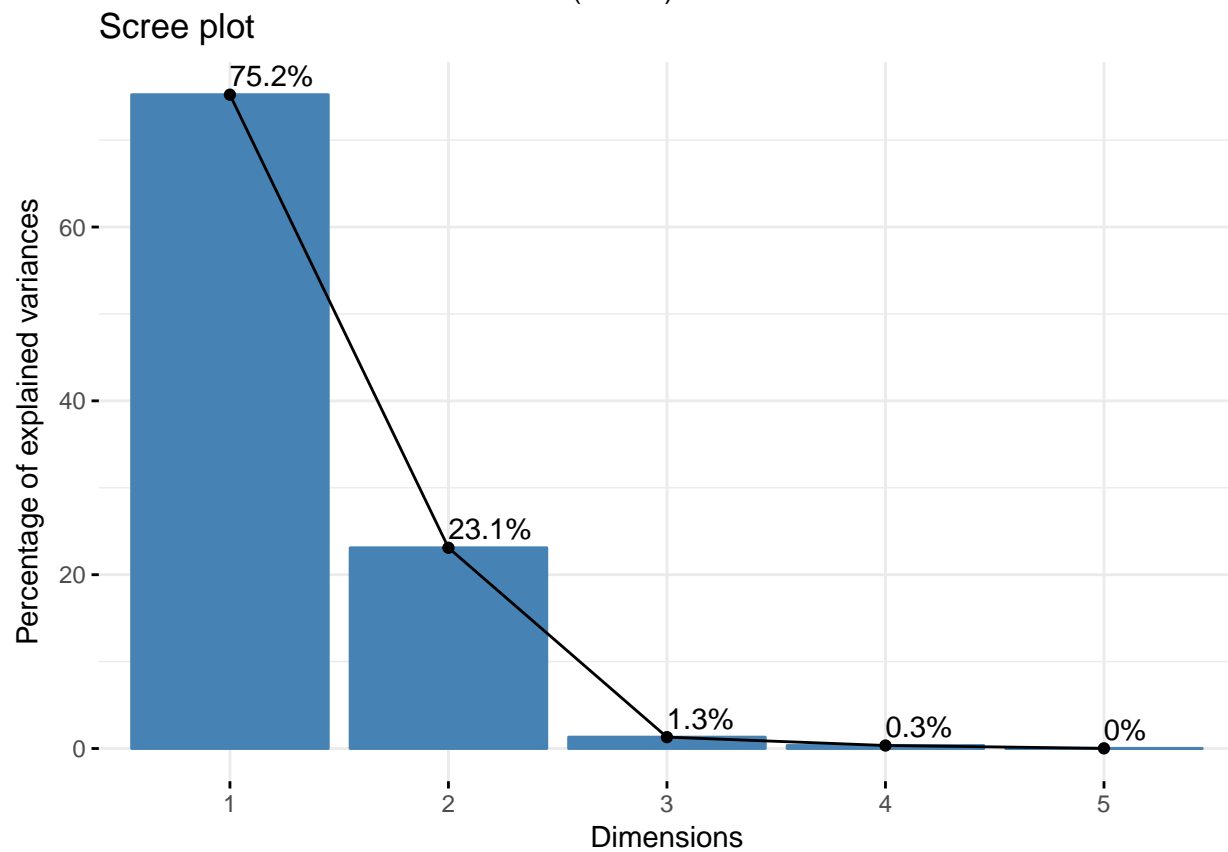
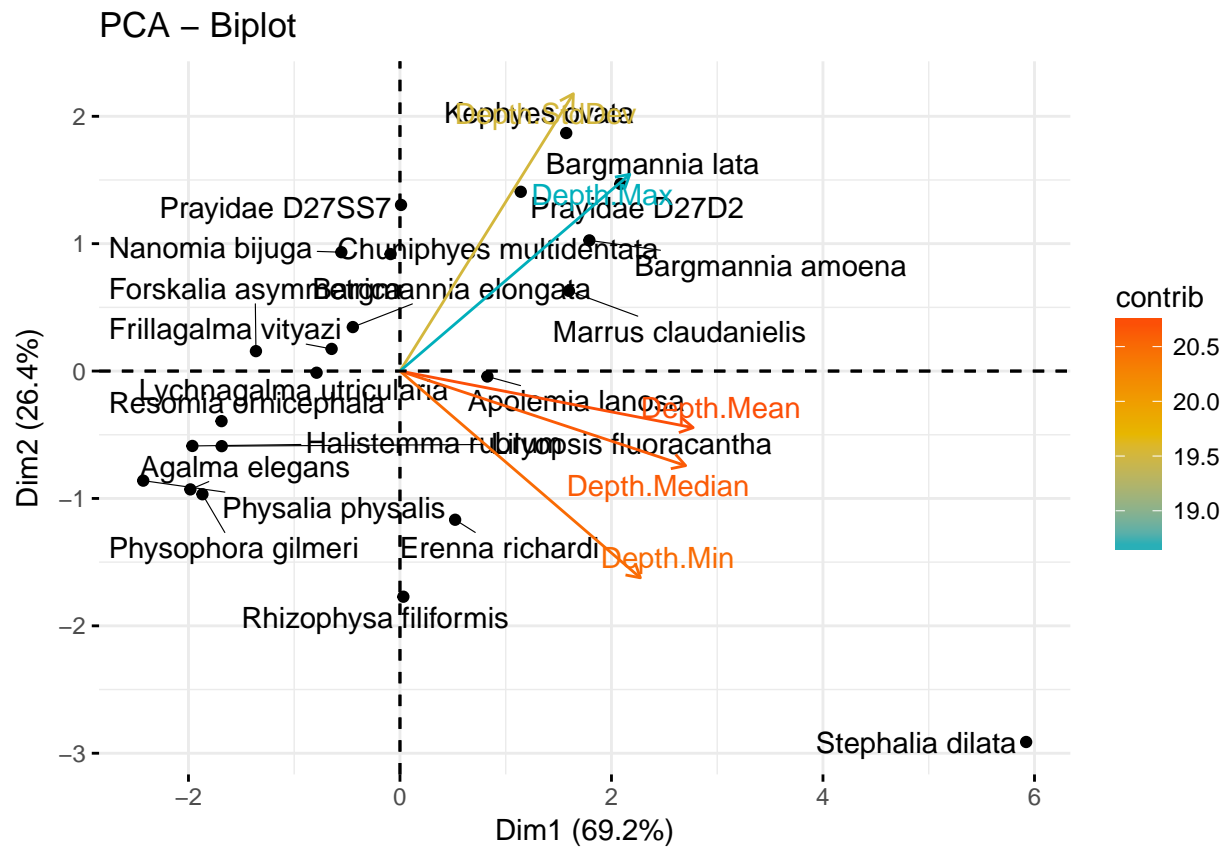
```
## Pneumatophore          0.001      -4.0370321
```

Phylogenetic signal in VARS bathymetrics

```
##
## Call:
## physignal(A = dpruned_data[, c(14, 15, 16, 18, 19)], phy = dpruned_tree)
##
##
##
## Observed Phylogenetic Signal (K): 0.7424
##
## P-value: 0.039
##
## Based on 1000 random permutations
##
##          K PIC.variance.obs PIC.variance.rnd.mean
## Depth.Median 0.7830816      797529.1      1276559.4
## Depth.Mean   0.7388410      941754.2      1453919.6
## Depth.StdDev 0.5929636      136382.4      164134.2
## Depth.Max    0.7181495      3265732.2      4754543.8
## Depth.Min    0.8396274      723182.9      1258465.5
##
##          PIC.variance.P PIC.variance.Z
## Depth.Median      0.065    -1.0427676
## Depth.Mean        0.057    -1.0214493
## Depth.StdDev      0.237    -0.7314187
## Depth.Max         0.059    -1.4636342
## Depth.Min         0.091    -0.9867170
```

Phylogenetic PCA for bathymetrics

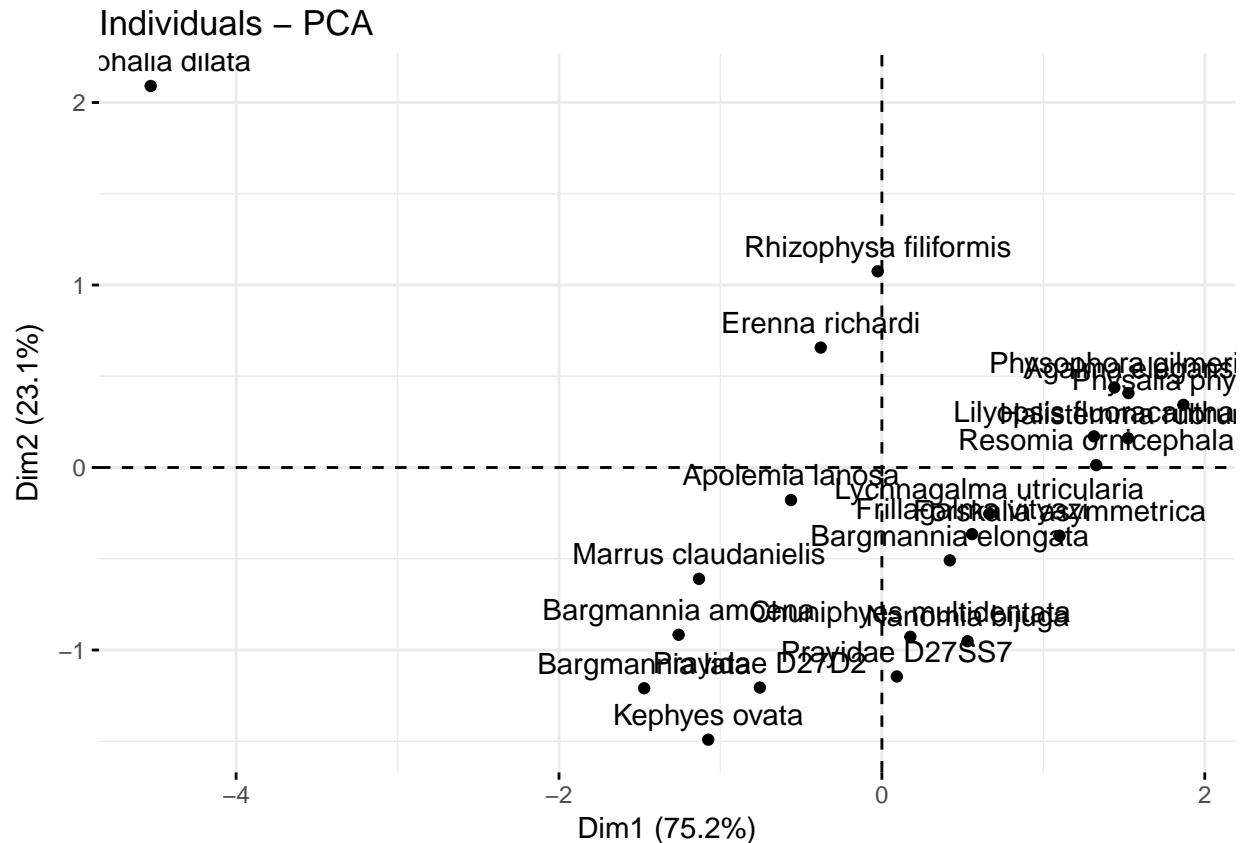




A bar chart titled 'Contributions (%)' on the y-axis. The x-axis lists five depth metrics: Depth.Mean, Depth.Median, Depth.Min, Depth.Max, and Depth.StdDev. The y-axis has major ticks at 0, 10, and 20. A horizontal red dashed line is drawn at the 20% mark. The bars are blue. Depth.Mean is the highest at approximately 28%, followed by Depth.Median at approximately 26%. Depth.Min is at approximately 19.5%, Depth.Max at approximately 15%, and Depth.StdDev is the lowest at approximately 11.5%.

Depth Metric	Contribution (%)
Depth.Mean	28
Depth.Median	26
Depth.Min	19.5
Depth.Max	15
Depth.StdDev	11.5

[illegible]



Phylogenetic ANOVA for depth

Each phylogenetic ANOVA compares variance of depth (continuous variable) within and between groups clustered by their categorical biological traits.

```
## [1] "Depth vs Sex Distribution"

## $F
## [1] 10.48139
##
## $Pf
## [1] 0.081
##
## $T
##           Dioecious Monoecious
## Dioecious  0.000000   3.237497
## Monoecious -3.237497   0.000000
##
## $method
## [1] "holm"
##
## $Pt
##           Dioecious Monoecious
## Dioecious    1.000    0.081
## Monoecious    0.081    1.000
## [1] "Depth vs Nectosome"
```

```

## $F
## [1] 0.2358588
##
## $Pf
## [1] 0.784
##
## $T
##      0      1
## 0 0.000000 -0.485653
## 1 0.485653  0.000000
##
## $method
## [1] "holm"
##
## $Pt
##      0      1
## 0 1.000 0.784
## 1 0.784 1.000

## [1] "Depth vs Nectophore Types and Number"

## $F
## [1] 0.156464
##
## $Pf
## [1] 0.982
##
## $T
##
##           Multiple of one type None One of one type
## Multiple of one type           NA  NA              NA
## None                        NA  NA              NA
## One of one type             NA  NA              NA
## Two of one type             NA  NA              NA
## Two of two types            NA  NA              NA
##
##           Two of one type Two of two types
## Multiple of one type      NA              NA
## None                      NA              NA
## One of one type           NA              NA
## Two of one type           NA              NA
## Two of two types          NA              NA
##
## $method
## [1] "holm"
##
## $Pt
##
##           Multiple of one type None One of one type
## Multiple of one type           NA  NA              NA
## None                        NA  NA              NA
## One of one type             NA  NA              NA
## Two of one type             NA  NA              NA
## Two of two types            NA  NA              NA
##
##           Two of one type Two of two types
## Multiple of one type      NA              NA
## None                      NA              NA
## One of one type           NA              NA

```

```

## Two of one type          NA          NA
## Two of two types         NA          NA

## [1] "Depth vs Nectosome Position"

## $F
## [1] 0.237949
##
## $Pf
## [1] 0.909
##
## $T
##           Dorsal      None      Ventral
## Dorsal    0.0000000 0.2240508 -0.4988957
## None      -0.2240508 0.0000000 -0.5640384
## Ventral   0.4988957 0.5640384  0.0000000
##
## $method
## [1] "holm"
##
## $Pt
##           Dorsal None Ventral
## Dorsal         1    1      1
## None           1    1      1
## Ventral        1    1      1

## [1] "Depth vs Palpons"

## $F
## [1] 0.05567054
##
## $Pf
## [1] 0.888
##
## $T
##           0      1
## 0  0.0000000 0.2359461
## 1 -0.2359461 0.0000000
##
## $method
## [1] "holm"
##
## $Pt
##           0      1
## 0  1.000 0.888
## 1  0.888 1.000

## [1] "Depth vs Tentilla"

## $F
## [1] 0.06009463
##
## $Pf
## [1] 0.856
##
## $T
##           0      1

```

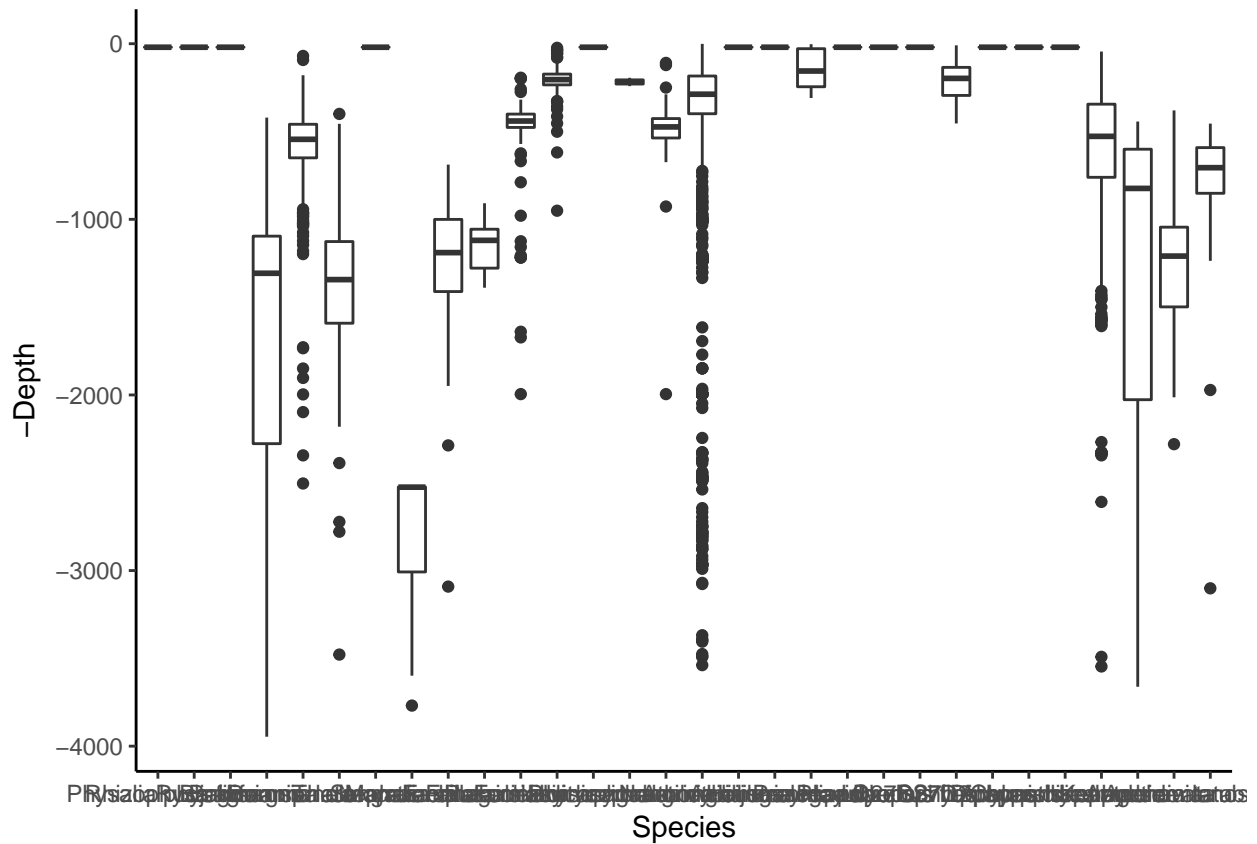
```
## 0 0.0000000 -0.2451421
## 1 0.2451421 0.0000000
##
## $method
## [1] "holm"
##
## $Pt
##      0      1
## 0 1.000 0.856
## 1 0.856 1.000
##
## [1] "Depth vs Pneumatophore"
##
## $F
## [1] 0.1796993
##
## $Pf
## [1] 0.817
##
## $T
##      0      1
## 0 0.0000000 -0.4239096
## 1 0.4239096 0.0000000
##
## $method
## [1] "holm"
##
## $Pt
##      0      1
## 0 1.000 0.817
## 1 0.817 1.000
```

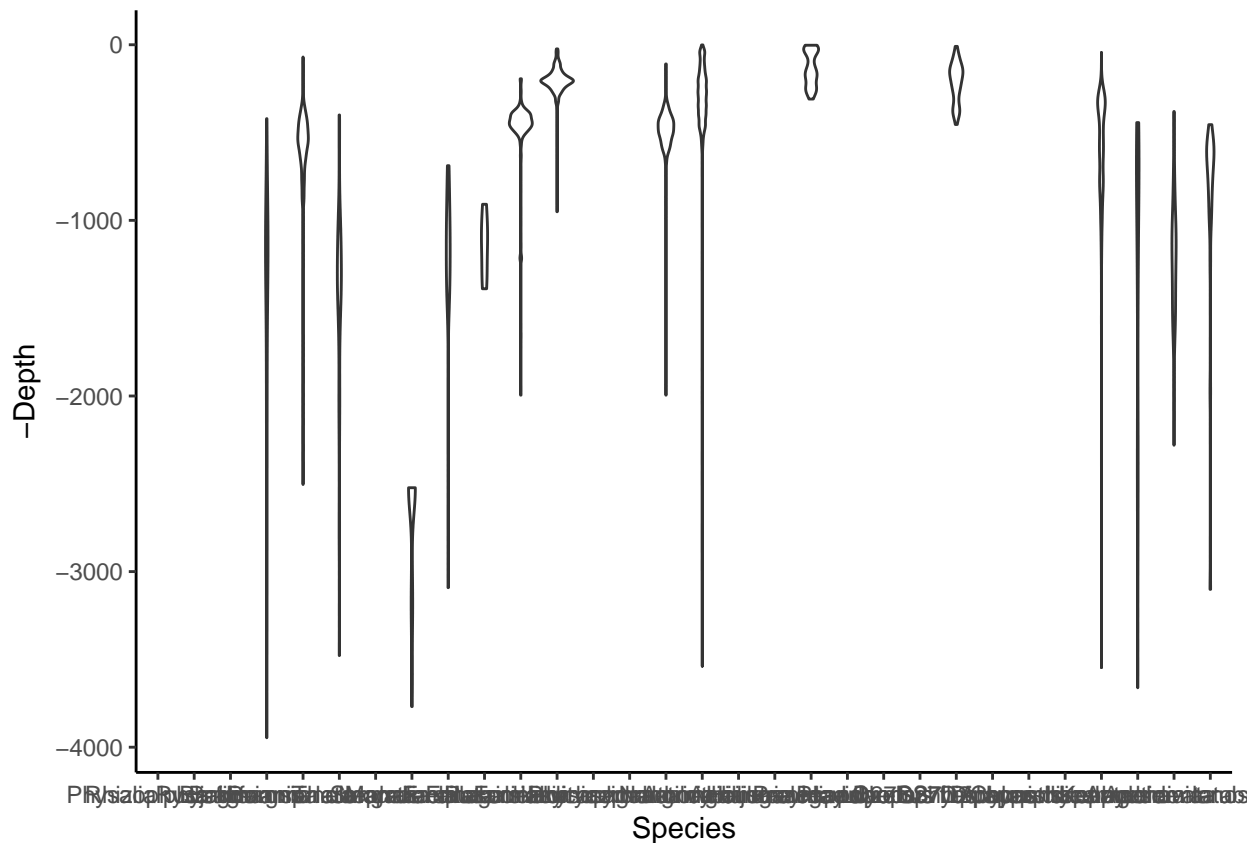
PGLS - Sex distribution

```
## -----
## | **Warning: |
## |   User reports suggest that this method may frequently |
## |   fail to find the ML solution. Please use with caution. |
## |-----|
##
## Call:
## phylolm(formula = depth_median ~ dp_sex, data = as.data.frame(cbind(depth_median,
##   dp_sex)), phy = dpruned_tree, model = "BM", measurement_error = TRUE,
##   boot = 100)
##
##      AIC logLik
## 347.7 -169.9
##
## Parameter estimate(s) using ML:
## sigma2: 217361.9
## sigma2_error: 142822
##
## Coefficients:
## (Intercept)      dp_sex
##    192.7735    958.4204
```

```
## Generalized least squares fit by REML
##   Model: dp_sex ~ depth_median
##   Data: NULL
##   Log-restricted-likelihood: -20.52555
##
## Coefficients:
##   (Intercept) depth_median
## 0.0978229509 0.0004267556
##
## Degrees of freedom: 22 total; 20 residual
## Residual standard error: 0.4176998
```

VARS data barplot code





Software versions

This manuscript was computed on Tue Nov 21 16:05:26 2017 with the following R package versions.

R version 3.4.1 (2017-06-30)

Platform: x86_64-apple-darwin15.6.0 (64-bit)

Running under: macOS Sierra 10.12.2

Matrix products: default

```
BLAS: /Library/Frameworks/R.framework/Versions/3.4/Resources/lib/libRblas.0.dylib
```

```
LAPACK: /Library/Frameworks/R.framework/Versions/3.4/Resources/lib/libRlapack.dylib
```

locale:

[1] en_GB.UTF-8/en_GB.UTF-8/en_GB.UTF-8/C/en_GB.UTF-8/en_GB.UTF-8

```
attached base packages:
```

```
[1] grid      parallel  stats      graphics  grDevices  utils      datasets
```

```
[8] methods base
```

other attached packages:

[1]	bindrcpp_0.2	phylolm_2.5	geomorph_3.0.5	rgl_0.98.1
[5]	adephylo_1.1-10	ade4_1.7-8	phylobase_0.8.4	geiger_2.0.6
[9]	phangorn_2.2.0	phytools_0.6-20	picante_1.6-2	nlme_3.1-131
[13]	vegan_2.4-4	lattice_0.20-35	permute_0.9-4	ape_4.1
[17]	hutan_0.5.0	FactoMineR_1.38	factoextra_1.0.5	gridExtra_2.3
[21]	seriation_1.2-2	fields_9.0	maps_3.2.0	spam_2.1-1

[25]	dotCall64_0.9-04	ggtree_1.8.2	treeio_1.0.2	cowplot_0.8.0
[29]	xtable_1.8-2	jsonlite_1.5	knitr_1.17	digest_0.6.12
[33]	magrittr_1.5	forcats_0.2.0	stringr_1.2.0	dplyr_0.7.4
[37]	purrr_0.2.3	readr_1.1.1	tidyr_0.7.1	tibble_1.3.4
[41]	ggplot2_2.2.1	tidyverse_1.1.1		

loaded via a namespace (and not attached):

[1]	readxl_1.0.0	uuid_0.1-2
[3]	backports_1.1.1	fastmatch_1.1-0
[5]	plyr_1.8.4	igraph_1.1.2
[7]	lazyeval_0.2.0	sp_1.2-5
[9]	splines_3.4.1	rncl_0.8.2
[11]	foreach_1.4.3	htmltools_0.3.6
[13]	viridis_0.4.0	gdata_2.18.0
[15]	cluster_2.0.6	gclus_1.3.1
[17]	modelr_0.1.1	gmodels_2.16.2
[19]	prettyunits_1.0.2	jpeg_0.1-8
[21]	colorspace_1.3-2	rvest_0.3.2
[23]	ggrepel_0.7.0	haven_1.1.0
[25]	bindr_0.1	survival_2.41-3
[27]	iterators_1.0.8	glue_1.1.1
[29]	registry_0.3	gtable_0.2.0
[31]	seqinr_3.4-5	kernlab_0.9-25
[33]	prabclus_2.2-6	DEoptimR_1.0-8
[35]	scales_0.5.0	mvtnorm_1.0-6
[37]	DBI_0.7	Rcpp_0.12.13
[39]	plotrix_3.6-6	viridisLite_0.2.0
[41]	progress_1.1.2	spdep_0.6-15
[43]	flashClust_1.01-2	foreign_0.8-69
[45]	subplex_1.4-1	bold_0.5.0
[47]	mclust_5.3	deSolve_1.20
[49]	stats4_3.4.1	animation_2.5
[51]	htmlwidgets_0.9	httr_1.3.1
[53]	gplots_3.0.1	fpc_2.1-10
[55]	modeltools_0.2-21	pkgconfig_2.0.1
[57]	reshape_0.8.7	XML_3.98-1.9
[59]	flexmix_2.3-14	deldir_0.1-14
[61]	nnet_7.3-12	crul_0.4.0
[63]	tidyselect_0.2.0	labeling_0.3
[65]	rlang_0.1.2	reshape2_1.4.2
[67]	munSELL_0.4.3	cellranger_1.1.0
[69]	tools_3.4.1	broom_0.4.2
[71]	evaluate_0.10.1	yaml_2.1.14
[73]	robustbase_0.92-7	caTools_1.17.1
[75]	dendextend_1.5.2	mime_0.5
[77]	whisker_0.3-2	taxize_0.9.0
[79]	adeigenet_2.1.0	leaps_3.0
[81]	xml2_1.1.1	compiler_3.4.1
[83]	curl_2.8.1	clusterGeneration_1.3.4
[85]	RNeXML_2.0.7	stringi_1.1.5
[87]	highr_0.6	trimcluster_0.1-2
[89]	Matrix_1.2-11	psych_1.7.8
[91]	msm_1.6.4	LearnBayes_2.15
[93]	combinat_0.0-8	data.table_1.10.4

[95] bitops_1.0-6	httpuv_1.3.5
[97] R6_2.2.2	TSP_1.1-5
[99] KernSmooth_2.23-15	codetools_0.2-15
[101] boot_1.3-20	MASS_7.3-47
[103] gtools_3.5.0	assertthat_0.2.0
[105] rprojroot_1.2	mnormt_1.5-5
[107] diptest_0.75-7	mgcv_1.8-22
[109] expm_0.999-2	hms_0.3
[111] quadprog_1.5-5	coda_0.19-1
[113] class_7.3-14	rmarkdown_1.6
[115] rvcheck_0.0.9	ggpubr_0.1.5
[117] shiny_1.0.5	numDeriv_2016.8-1
[119] scatterplot3d_0.3-40	lubridate_1.6.0

References

- Beklemishev W.N. 1969. Principles of comparative anatomy of invertebrates. Edinburgh:Oliver & Boyd.
- Carré C. 1967. Le developpement larvaire d'Abylopsis tetragona. Cahiers de Biologie Marine. 8:185–193.
- Carré C., Carré D. 1991. A complete life cycle of the calycophoran siphonophore muggiaea kochi (will) in the laboratory, under different temperature conditions: Ecological implications. Philosophical Transactions of the Royal Society of London B: Biological Sciences. 334:27–32.
- Carré C., Carré D. 1995. Trait e de zoologie. anatomie, systématique, biologie. Paris:Masson.
- Carré D. 1969. Etude histologique du developpement de nanomia bijuga (chiaje, 1841), siphonophore physonecte, agalmidae. Cahiers de Biologie Marine. 10:325–341.
- Cartwright P., Nawrocki A.M. 2010. Character evolution in hydrozoa (phylum cnidaria). Integrative and Comparative Biology. 50:456–472.
- Dunn C., Pugh P., Haddock S. 2005. Molecular Phylogenetics of the Siphonophora (Cnidaria), with Implications for the Evolution of Functional Specialization. Systematic biology. 54:916–935.
- Dunn C.W., Howison M., Zapata F. 2013. Agalma: an automated phylogenomics workflow. BMC Bioinformatics. 14:330.
- Dunn C.W., Wagner G.P. 2006. The evolution of colony-level development in the siphonophora (cnidaria: Hydrozoa). Development genes and evolution. 216:743–754.
- Lartillot N., Lepage T., Blanquart S. 2009. PhyloBayes 3: A bayesian software package for phylogenetic reconstruction and molecular dating. Bioinformatics. 25:2286–2288.
- Lartillot N., Philippe H. 2004. A bayesian mixture model for across-site heterogeneities in the amino-acid replacement process. Molecular Biology and Evolution. 21:1095–1109.
- Mackie G., Pugh P., Purcell J. 1988. Siphonophore biology. Advances in marine biology. 24:97–262.
- Pugh P. 1983. Benthic siphonophores: A review of the family rhodaliidae (siphonophora, physonectae). Philosophical Transactions of the Royal Society of London, B. 301:165–300.
- Studies on physalia physalis (l.). part 1. natural history and morphologyDiscovery Reports. 30:301–368.
- Totton A.K., Bargmann H.E. 1965. A synopsis of the siphonophora. British Museum (Natural History).
- Yu G., Smith D.K., Zhu H., Guan Y., Lam T.T.-Y. 2016. ggtree: an r package for visualization and annotation of phylogenetic trees with their covariates and other associated data. Methods in Ecology and Evolution.

Species	Mean insert size (bp)	Insert size standard deviation	Number of read pairs	Percent kept after rRNA removal	Percent kept after assembly	Adapter fails	Quality fails	Base Composition fails	Total assembled transcripts	Coding transcripts
Marrus claudanielis	253.03	53.30	35866092	96.8	62.1	113298	15594637	4981676	105439	22511
Apolemia rubriversa	290.81	80.64	19228660	91.7	77.8	40594	5179800	516100	87701	17540
Chuniphyces multi-dentata	284.46	35.74	17999147	77.0	74.3	24263	4941872	335297	84341	22084
Apolemia sp	167.41	53.46	16761717	81.3	79.4	1332063	3062035	41943	51470	14752
Apolemia lanosa	167.74	55.30	18444476	96.4	80.9	923922	3882968	439569	70184	15579
Bargmannia elongata	271.43	40.17	40008913	79.8	78.5	342825	8084832	2017709	152019	23661
Diphyes dispar	223.14	58.73	80000000	78.7	63.4	14412120	21322624	690159	210406	50868
Aiptasia pallida	183.18	53.88	74558341	98.4	79.3	210730	23826421	307520	83950	33523
Stephalia dilata	267.82	43.33	30953585	98.0	63.9	86068	15731787	1435119	107925	23984
Physalis physalis	233.10	54.37	36481773	96.6	88.5	18553	5491979	259497	74994	23705
Bargmannia amoena	261.57	53.77	20195498	84.6	80.1	1049110	3996085	274520	66726	17975
Frillagalma vityazi	283.11	44.91	79902051	54.0	70.4	668400	13591301	5558767	181508	29293
Alatina alata	173.96	60.33	96259870	52.1	77.9	1236251	15771112	468662	166584	28743
Clytia hemisphaerica									11476	6642
Ectopleura larynx	229.05	37.75	109024653	95.9	74.6	432309	40629127	897590	84034	28015
Athorybia rosacea	221.16	93.65	28696930	99.9	86.9	691916	4026467	633700	100839	24543
Forskalia asymmetrica	259.42	35.04	25275184	58.9	65.1	41922	7463840	841930	82483	18419
Prayidae D27D2	267.32	45.59	38233199	85.2	66.4	59773	15338562	1878732	144909	28065
Lilyopsis fluoracantha	259.39	39.08	51855968	76.5	65.3	72416	19809124	1388875	114662	29854
Hydractinia symbiolongicarpus	175.22	57.84	60462724	49.8	85.2	162430	6678373	124392	71450	24639
Rhizophysa filiformis	269.74	46.52	26937827	92.5	65.3	66010	13238701	361376	110109	24833
Agalma elegans	238.94	57.54	40007833	99.6	86.0	31957	7177806	748977	122053	26601
Chelophyes appendiculata	275.93	39.43	21103284	89.0	74.2	63548	6777022	344708	110612	32309
Prayidae D27SS7	303.39	50.83	25233164	66.7	65.6	39061	8616289	347189	94917	24211
Rudjakovia sp	213.88	89.71	20582477	99.1	79.7	489520	3936086	1546686	91695	24184
Abylopsis tetragona	292.16	38.32	21575176	73.3	73.8	38764	5759144	370604	102946	25268
Nematostella vectensis									26511	18080
Hippopodius hippopus	266.99	45.11	35638254	84.5	66.3	56152	15490291	535026	137341	35031
Physophora gilmeri	214.97	93.78	19847377	99.3	81.3	936617	3464079	1007839	52639	17381
Bargmannia lata	266.71	62.80	16984483	98.7	71.1	3118496	4227140	868584	59051	16451
Nanomia bijuga	296.69	44.20	39983229	85.7	75.36	155093	10854240	795226	165792	28927
Erenna richardi	291.53	36.76	29776547	64.2	66.6	39775	8958200	1245523	89423	18236
Physonect sp	261.09	35.96	38243543	24.3	66.7	12494	4517982	274838	57746	12596